Boulder transport and wave height of a seventeenth century South China Sea tsunami on Penghu Islands, Taiwan

Neng-Ti Yu [1]*, Cheng-Hao Lu [2], I-Chin Yen[3], Jia-Hong Chen[4], Jiun-Yee Yen[5], Shyh-Jeng Chyi [6]

[1] Center for General Education, National Tsing Hua University, 101, Sec. 2, Kuang-Fu Rd., Hsinchu City 300044, Taiwan; ntyu@mx.nthu.edu.tw
[2] Department of Tourism and Leisure, National Penghu University of Science and Technology, 300, Liuhe Rd., Magong City, Penghu County 880011, Taiwan; luch@gms.npu.edu.tw
[3] Graduate Institute of Applied Geology, National Central University, 300, Zhongda Rd., Zhongli Dist., Taoyuan City 320317, Taiwan; ichin.yen@gmail.com
[4] Department of Natural Resources and Environmental Studies, National Dong Hwa University, 1, Sec. 2, Da Hsueh Rd., Shoufeng, Hualien 974301, Taiwan; jiahong1017@gmail.com
[5] Department of Natural Resources and Environmental Studies, National Dong Hwa University, 1, Sec. 2, Da Hsueh Rd., Shoufeng, Hualien 974301, Taiwan; jyyen@gms.ndhu.edu.tw
[6] Department of Geography, National Kaohsiung Normal University, 116, Heping 1st Rd., Lingya District, Kaohsiung City 802561, Taiwan, chyisj@nknu.edu.tw

Correspondence to: Neng-Ti Yu (ntyu@mx.nthu.edu.tw)

Abstract. The South China Sea faces widespread tsunami risks from diverse sources, including trench megathrusts, intraplate earthquakes, and landslides. However, historical and geological records are scarce to constrain worse-case simulations. The cliff-top basalt boulders on the Penghu Islands in the Taiwan Strait provide wave estimates from incipient motion formulas and stratigraphic links to the probable sources. Calibrating for ancient local sea level and 100-year surge indicates that storm waves in the shallow interisland bathymetry only enable boulder sliding–rolling below the 2.5 m high cliff. A minimum tsunami wave height of ~3.2 m is necessary for cliff-top overflow to exceed boulder height and terminal rolling before deposition. Coeval gravels in two other outcrops also record the time and extent of tsunami deposition with beach-derived bioclasts, stranded pumices, sharp base, matrix support, poor sorting, and elevations surpassing the 100-year surge. These gravels mark local minimum wave run-ups reaching 2.4–4.0 m above sea level. The 1575–1706 radiocarbon age of the studied boulder suggests a probable tie to the disastrous 1661 earthquake in southwest Taiwan and the megathrust source in the northern Manila Trench.

1 Introduction

Devastating wave impacts, such as those associated with the annual typhoons, pose a constant threat along the coasts of the South China Sea. Despite being often overlooked because of extended recurrence, tsunamis present severe risks in the

已删除: hu

已删除: hu

已删除:

已删除: ….The widespread tsunami risks in the …outh China Sea faces widespread tsunami risks fromhave…diverse sourcesorigins…includingfrom…trench megathrusts, to …ntraplate earthquakes, andor…landslides. However,and remain poorly understood due to the scarce…historical and geological records are scarce to constrain worse-case simulations. The cliff-top paleotsunami gravels and …asalt boulders on the Penghu Islands in the Taiwan Strait provideesent facies constraints on sediment transport,…wave estimates from incipient motion formulas,…and stratigraphic links to the probable sources. The boulders are supported by a pumice-bearing mud matrix that reflects a suspension-rich turbulent flow process and the typical rolling–saltation transport that results from bore-like waves.…Calibrating for ancient local sea level height…and 100 …00-year surge indicates that the…storm waves that are likely to form …n the shallow interisland bathymetry only enable boulder sliding–rolling belowand are incapable of…the 2.5 m high cliff-top deposition… The… estimated…minimum height of …sunami wave heights…of ~3.2 m is necessaryis also insufficient and needs to add to 3.0 m…high …or a minimum …liff-top overflow to exceed boulder heightof 0.5 m depth…andfor…terminal rolling before deposition. Coeval gravels in two other outcrops also record the time and extent of tsunami deposition,…withand…are characterized by …each-derived bioclasts and… stranded pumices, sharp base, matrix support, poor sorting, and elevations surpassreach…ng above …he 100 …00-year surge. These gravels mark the …ocal minimum wave run-ups, and …eaching 2.4–4.0 m above sea level. The 1575–1706 radiocarbon age of the studied boulder suggests a probable tie to the disastrous 1661 earthquake in southwestthe SW…Taiwan Orogen ... [1]

已删除: are…a constant threat alongt…the coasts of the South China Sea. Despite beingThe potentially hazardous tsunami waves are, however,…often overlooked because of extended recurrence, tsunamisalthough ubiquitous…presentand…severediverse…riskource… ... [2]

region due to their ubiquitous and diverse sources, such as the Manila Trench in the east, intraplate seismicity in the north–west, and steep slopes with pronounced landslide potential throughout the area (Fig. 1a; Goff et al., 2020; Terry et al., 2017).

To take proper precautions against tsunamis, numerous forward hydrodynamic simulations have been generated to illustrate the worst-case scenarios of tsunami wave generation, propagation, and inundation resulting from geological sources in the area (e.g., Qiu et al., 2019; Li et al., 2019; Li et al., 2016; Li et al., 2015; Okal et al., 2011; Wu and Huang, 2009; Megawati et al., 2009; Liu et al., 2022). However, the effectiveness of these simulations has not been assessed due to limited data from modern observation, historical accounts, and geological evidence. Modern tsunamis originating in the South China Sea have been insignificant, including those that followed the 1994 and 2006 earthquakes, with wave heights reaching less than 60 cm (Fig. 1a; Central Weather Bureau, 2022). Historical accounts of events such as the 1604, 1640, and 1661 earthquakes are often vague and only describe seawater overflow, which is not necessarily indicative of a tsunami (Lau et al., 2010; Keimatsu, 1963. (in Japanese with English abstract); Nakamura, 1935. (in Japanese); Lei and Ou, 1991. (in Chinese with English abstract)). Accounts of the late 18th century tsunami in SW Taiwan remain controversial in terms of several aspects, including the exact date (1781 or 1782), the death toll (one or tens of thousand), the extent of inundation (tens of meters or tens of kilometers inland), and whether the event was coupled with an earthquake (Li et al., 2015; Lau et al., 2010; Liu et al., 2022). Recent geological investigations have identified three event layers from the fourth to the 16th centuries across the South China Sea (Lu et al., 2019; Sun et al., 2013; Ramos et al., 2017; Yang et al., 2019). However, these findings provide limited information for an accurate quantitative evaluation of the landward inundation, wave heights, and run-ups.

In this study, the Penghu Islands in the Taiwan Strait, located in the northeast South China Sea, were selected for further geological investigation due to their close proximity to potential tsunami sources and the previous discovery of three paleotsunami deposits (Fig. 1a; Lu et al., 2019). A new and younger marine gravel deposit from the 17th century was identified at several coastal localities. Cliff-top basalt boulders are present in one of the sites, providing crucial clues for estimating wave heights and periods during sediment transport and deposition. The matrix-supported boulders and the fine-grained matrix are well preserved and represent key facies for understanding transport modes and flow processes.

To better distinguish between tsunami and typhoon wave processes in the gravel deposit and reduce uncertainties in the wave estimation, multiple previously modified incipient motion formulas were utilized in conjunction with the constraints obtained from the facies, stratigraphy, geomorphology, and modern observations (Nandasena, 2020; Cox et al., 2020; Kennedy et al., 2021; Barbano et al., 2010; Lorang, 2011; Nandasena et al., 2011; Pignatelli et al., 2009; Nott, 2003; Nandasena et al., 2022). The modifications and constraints considered various factors, such as the virtual boulder dimensions, maximum lifting surface, sediment sources, transport distances, shore slope angle, bathymetry, ancient local sea level, modern records of typhoon waves, surges, and tsunamis, as well as estimated heights of 100-year significant waves and surges. Radiocarbon dating facilitated accurate determination of the depositional age of the boulders, allowing for correlation with probable historical typhoon and tsunami events. This study aimed to delineate quantitative and qualitative estimations of wave extent and boulder transport during impact, ultimately enhancing our understanding of tsunami risks by comparing the results with those obtained in previous simulations.

已删除: ,…throughoutare…found all over …he aregion ... [3]

已删除: that…illustrate the worst-case scenarios of tsunami wave generation, propagation, and inundation as a …esulting o…rom the …eological sources in the area (e.g., Qiu et al., 2019; Li et al., 2019; Li et al., 2016; Li et al., 2015; Okal et al., 2011; Wu and Huang, 2009; Megawati et al., 2009; Liu et al., 2022). However, the effectivenessmitigation value…of these simulations has not been assessed due to limitedinsufficient…dataconstraints…from modern observation, historical accounts, and geological evidence. The m…odern tsunamis that have …riginatinged…in the South China Sea have been insignificant, including those that followed the 1994 and 2006 earthquakes, with wave heights reaching less than 60 cm (Fig. 1a; Central Weather Bureau, 2022). Historical accounts of events such as the 1604, 1640, and 1661 earthquakes are oftenusually…vague and only describe seawater overflow, which is not necessarily indicativerelated…ofto…a tsunami (Lau et al., 2010; Keimatsu, 1963. (in Japanese with English abstract); Nakamura, 1935. (in Japanese); Lei and Ou, 1991. (in Chinese with English abstract)). Accounts of the late 18th century tsunami in SW Taiwan remain controversial in terms of several aspects, including the exact dateage…(1781 or 1782), the death toll (one or tens of thousand), the extent of the extent of …nundation (tens of meters or tens of kilometers inland), and whether the event was coupled with an earthquake (Li et al., 2015; Lau et al., 2010; Liu et al., 2022). Recent geological investigations have identified three event layers from the four4…h to the 16th centuries across the South China Sea (Lu et al., 2019; Sun et al., 2013; Ramos et al., 2017; Yang et al., 2019).…However,However,…these findings provide limitedfurther…information is required ... [4]

已删除: NE…South China Sea, were selected for further geological investigation duebecause…tof…their close proximity to potentialseveral…tsunami sources and the previous discovery of three paleotsunami deposits in the area…(Fig. 1a; Lu et al., 2019),…with a… new and younger marine gravel deposit from the 17th century was identified at several coastal localities. C. The c…iff-top basalt boulders at one of the coastal exposure sites…are present in one of the sites, providinge…crucial clues for estimating wave heights and periods during sediment transport and deposition, and have been considered in this study for the first time… The matrix-supported boulders and the fine-grained matrix are well preserved and outcropped,…representleading to a unique situation in which…key key …acies for understandingcan be observed and used to constrain both ... [5]

已删除: M…odifications and constraints considered various factors,include…such as the virtual boulder dimensions, maximum lifting surface, fundamental physics… sediment sources, transport distances, shore slope angle, bathymetry, ancient local sea level, modern records of typhoon waves, surges, and tsunamis, as well asnd…estimated heights of 100 …00-year significant waves and surges. Radiocarbon dating facilitates… accurate determination of the depositional age of the boulders, and …llowings…for correlation with probable historical typhoon and tsunami events. Thise…study is …imed a…o delineapresen…ing… accurate …uantitative and qualitative estimations of wave extent and boulder transport during impact, ultimatelyand…enhancimprov ... [6]

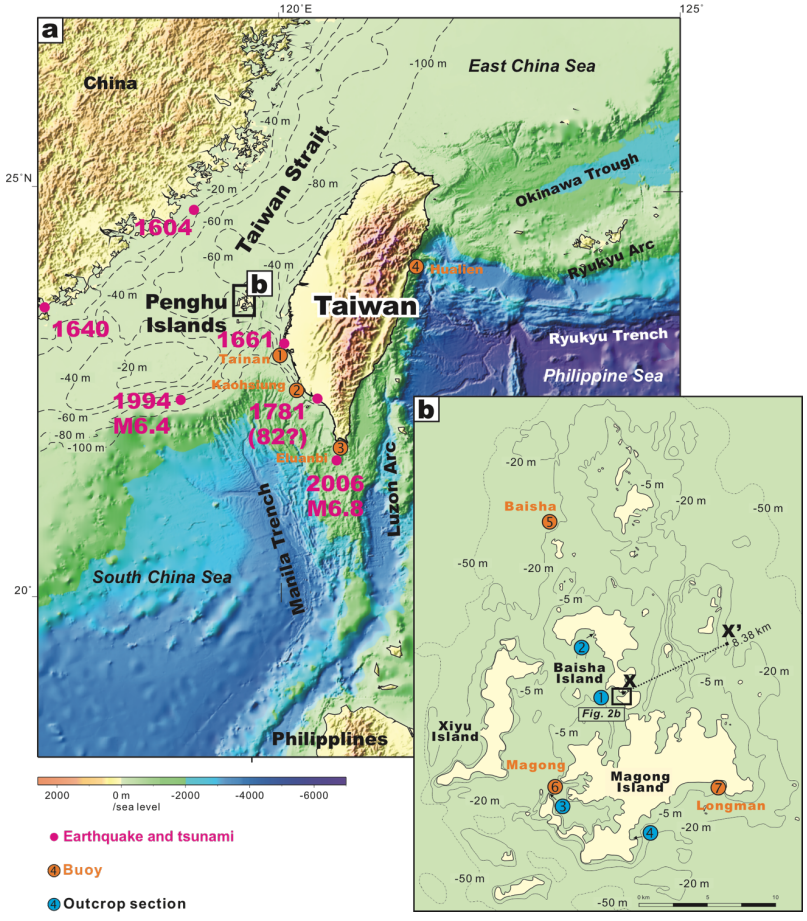

265

Figure 1: Geomorphology of the study area. (a) Regional map of Taiwan with earthquakes and tsunamis from the 17th century. The earthquake and tsunami events are based on Keimatsu (1963) and Central Weather Bureau (2022). (b) Penghu Islands and local bathymetry. X–X' transect manifests a bathymetric gradient of 20:8380.

已刪除: (Keimatsu, 1963; Central Weather Bureau, 2022)

已刪除: Map of

已刪除: with outcrop localities

已刪除: minor

2 Study area

The Taiwan Strait is a narrow and shallow channel located west of Taiwan, connecting the East and South China Seas, extending from northeast to southwest, with an average width of 180 km and an average water depth of 60 m (Fig. 1a). The southern part of the strait comprises the Penghu Islands, which consist of more than 90 volcanic islands made of Miocene basalt. These islands have an elevation of 10–20 m above sea level (a.s.l.) and are fringed by rocky shore terraces and platforms that reach a depth of 20 m offshore (Fig. 1b; Yen and Lee, 2017. (in Chinese with English abstract)). Although the Penghu area is not far from the active plate convergence zone at the orogenic island of Taiwan, it remains tectonically stable and is often used as a fixed reference point for geodetic studies (Yu et al., 1997). Accordingly, the local sea level in this area has been controlled by the global sea level fluctuations, falling at approximately 5.1 cm per century from a 2.4 m highstand since 4.7 ka (Chen and Liu, 1996).

Both Taiwan and the Taiwan Strait are subjected to powerful typhoons, which have set wave height and period records at the Paisha buoy in the Penghu Islands and the Tainan, Kaohsiung, Elaunbi, and Hualien buoys in southern and eastern Taiwan (Table 1, Fig. 1a–b; Central Weather Bureau, 2022). The estimated significant wave heights over 50- and 100-year periods have been available from the Paisha, Tainan, Kaohsiung, and Hualien buoys (Jiang et al., 2012. (in Chinese with English abstract), 2011. (in Chinese with English abstract); Chang, 2009. (in Chinese with English abstract)). In general, typhoon-induced waves are less intense in the Taiwan Strait due to its narrow, shallow, and tide-dominated nature, as shown by the maximum wave height of 65.8 m recorded at the Paisha buoy, compared to the 11.9–17.8-m maxima observed at the other buoys adjacent to deeper open water.

Modern and ancient typhoon surges from the 17th century have been prominent in the Penghu area, with a mesotidal range of 2.0–3.2 m (Hsu, 2007. (in Chinese); Central Weather Bureau, 2022). Notably, Typhoon Mitag in 2009 caused a surge with a maximum elevation of 1.8 m a.s.l. Between 1997 and 2021, 87 % of the 118 observed surges were with the range of 0.8–1.5 m a.s.l., with a mode of 1.1 m a.s.l. Ancient records document a surge of 1.2 m a.s.l. in 1683, as well as two surges reaching 1.5 m a.s.l. in 1832. In this study, the modern surge maximum of 1.8 m a.s.l. tentatively serves as an approximation for a 100-year surge.

The history of severe wave events at the Penghu Islands dates back to the thirteenth century, and no ancient tsunamis were recorded. The highest wave height associated with an earthquake-related tsunami occurred in 1994, measuring 0.4 m (Fig. 1a; Central Weather Bureau, 2022).

已刪除: ,…is a narrow and shallow channel locatedthat…lies north…est of Taiwan, connecting the East and South China Seas, extending from northeastNE…to southwestSW… with an average width of 180 km and an average dominant …ater depth of 20–8…0 m (Fig. 1a). The southern part of Penghu islands in…the southern …trait comprises the Penghu Islands, whichare…consistmposed…of more than 90 volcanic islandsunits…made of Miocene basalt. platform…These islandsand…have an elevation ofre…mainly …0–20 m above sea level (a.s.l.),…and are fringed by rocky shore terraces and platforms that reach a depth of 20 m offshore (Fig. 1b; Yen and Lee, 2017. (in Chinese with English abstract)). Although the Penghu area is not far from the active plate convergence zone at the orogenic island of Taiwan orogen… ithe region…remaini… tectonically stable and is often used as a fixed reference point for geodetic studiesreference…(Yu et al., 1997). Accordingly, T…he local sea level in this area has been controlled by the global sea level fluctuations, falling at approximately 5.1 cm per century from the Late Holocene in the region, decreasing…from a by ….4 m from a …ighstand sincemaximum…4.7 ka00 years ago to that observed in the present… ... [7]

已刪除: regularly …ubjected to powerful typhoons, which have setand several…wave height and period records have been set…at Paisha buoy in the Penghu Islands and the Tainan, Kaohsiung, Elaunbi, and Hualien buoys in southern and–…eastern Taiwan (Table 1, Fig. 1a–b; Central Weather Bureau, 2022). The estimated significant wave heights over 50- and 100-year periods haveare…been available from the Paisha, Tainan, Kaohsiung, and Hualien bB…oys (Jiang et al., 2012. (in Chinese with English abstract), 2011. (in Chinese with English abstract); Chang, 2009. (in Chinese with English abstract)). In general, typhoon-induced waves are less intense in the Taiwan Strait due to its narrow, shallow, and tide-dominated natureTaiwan Strait… as shown by the maximum wave height of 65.8 m recordedmaximum…at the Paisha (6.8 m)…buoy, compared toas compared to…the 11.9–17.8 …-m maxima observed observed …t the other buoys that are …djacent to de ... [8]

已刪除: Records of m…odern and ancient typhoon surges from the 17th century haveare…beenavailable…prominent infor…the Penghu area, with a mesotidal range of 2.0–3.2 m (Hsu, 2007. (in Chinese); Central Weather Bureau, 2022). Notably, Typhoon Mitag in 2009 causedA…amodern…surge with a maximum elevation of 1.8 m a.s.l. resulted from Typhoon Mitag in 2019….BetweenFrom…1997 andto…2021, 87 % of the 118 observed surges were with the range of 0.8–1.5 m a.s.l., with a mode of 1.1 m a.s.l. AA…cient records documentinclude…a surge of 1.2 m a.s.l. surge …n 1683, as well asnd…two surges that …eachinged…1.5 m a.s.l. in 1832. In this study, theA…modern surge maximum of 1.8 m a.s.l. is …entatively servesinferred to…as an approximation for athe…100 …00-year in this study ... [9]

已刪除: Records…of severe wave events at the the …enghu Islands datestart… back toin…the thirteenth century, and no ancient tsunamiss…wereere…recorded. The highest wave height associated with anmodern…earthquake-related tsunami occurred in 1994, measuring sets the wave height record at…0.4 m (Fig. 1a; Central Weather Bureau, 2022). ... [10]

格式化: 左右對齊, 縮排: 第一行: 1.27 公分, 行距: 1.5 倍行高

Table 1. Yearly and monthly wave records and estimated significant wave heights at buoys in the study area. For buoy locations, see Fig. 1a.

Time	Number of measurements	Max significant wave[1]				Probable significant wave	
		H	P	D	Date	50-year H	100-year H
Paisha (Penghu Islands; 2006–2021)							
Aug.	9,554	6.8	8.7	337	08/08/2015[2]	7.3[6]	
Oct./year	10,821	6.8	10.4	45	03/11/2011[3]		
Tainan (Qigu; 2006–2021)							
Aug./year	10,594	14.0	10.4	258	08/08/2015	11.6[7]	12.8[7]
Kaohsiung (Mituo; 2012–2021)							
Aug.	6,237	10.9	17.0	281	08/08/2015	10.0[8]	10.8[8]
Sep./year	6,662	12.2	23.2	236	14/09/2016[4]		
Elaunbi (2002–2021)							
Aug.	12,660	10.7	13.1	—	08/08/2009[5]		
Sep./year	11,868	17.8	13.1	168	14/09/2016		
Hualien (2002–2021)							
Aug./year	12,420	11.9	13.1	90	08/08/2015	15.7[8]	16.3[8]

H: wave height (m), P: wave period (s), D: wave direction (degrees).
[1]Wave statistics from buoys at a depth of 20–40 m (Central Weather Bureau, 2022), [2]Typhoon Soudelor, [3]Atmospheric pressure low, [4]Super typhoon Meranti, [5]Typhoon Morakot, [6]Chang (2009), [7]Jiang et al. (2012), [8]Jiang et al. (2011).

3 Materials and methods

3.1 Cliff-top boulder and incorporative hydrodynamic approach

The cliff-top basalt boulder is located in outcrop Chungtun-1, which lies on the southern shore of a narrow and shallow interisland channel known as Chungtun Channel (Fig. 2a). The channel is 350–500 m wide and ~2.5 m deep (Fig. 2b–c).

已删除: B
已删除: can be
已删除: n
已删除: in
已删除: Observation
格式化: 靠左
已删除: H
已删除: Period
50
已删除: s
已删除: 100
已删除: s
已删除: /08/08
已删除: /10/03
已删除: /08/08
已删除: /08/08
已删除: /09/14
已删除: /08/08
已删除: /09/14
已删除: /08/08
格式化: 缩排: 左: 0 公分, 凸出: 2.84 字元
已删除: studied
已删除: found
已删除: CT
已删除: ,
已删除: denoted the
已删除: T
已删除: in
已删除: largely

The largest boulder clast, hereafter referred to as 'Chungtun-1 boulder,' was selected for analysis due to its significantly larger size compared to the others in the outcrop (Fig. 3a). These boulder clasts form a cluster in a mud-matrix-supported gravel layer that is laterally continuous and gradually thins out upward from 2.5 to 4.0 m a.s.l. This layer is referred to as 'Chungtun-1 layer' (Fig. 3a). Marine shells and rounded pumice pebbles are abundant in the matrix and also on the channel beach (Fig. 3b); however, they are absent in the underlying basalt basement and basal soil as well as the overlying angular-gravel colluvium. Accordingly, it is assumed that the cliff-top boulder and gravel layer have a marine sediment origin.

The metrics of the Chungtun-1 boulder were measured using Autodesk Meshmixer and Context Capture; the measurements include a density of 2.91 g cm^{-3}, a volume of 0.73 m^3 volume, a mass of 2.12 t, an axis length og 1.71–0.69 m, and a projected surface area of 1.66–1.01 m^2 (Fig. 3c). The boulder shape is angular, indicating its origin from a joint-bounded source in the intertidal–subtidal zone since subaerial spheroidal weathering and rock residue are well developed across the islands, including the basalt cliff of outcrop Chungtun-1 (Fig. 3a). There is an intertidal rock exposure at 0.5 m below sea level, which exhibits well-developed joint fractures and rock debris similar in size and shape to the boulder clasts of the Chungtun-1 outcrop (Fig. 3a and d). This rock exposure forms a wave-cut bench and marks an inflection point on the shore profile, indicating a transport distance of 31.7 m to the Chungtun-1 outcrop (Fig. 2; Lorang, 2011). A transect through the outcrop to the probable source and the deepest channel shows shore slope angles of 21.5° in the supratidal zone, 3.6° in the beach–intertidal zone, and 0.01° in the subtidal zone (YY' in Fig. 2c).

The incorporative hydrodynamic approach used in this study involves two main procedures: (1) an estimation of the minimum wave heights and periods required for the initiation of transport of the Chungtun-1 boulder using the modified incipient motion formulas, and (2) distinguishing between the typhoon and tsunami wave origins by comparing the estimation results with various wave sources such as modern and ancient tsunami waves, typhoon waves, 100-year significant waves, and 100-year surge (Cox et al., 2020). The comparison also integrates the constraints from the geomorphology, bathymetry, ancient local sea level, and the ratio of wave height to water depth at the wave break. The wave height/flow depth estimate is delineated a step further from flow velocity, as it has been deemed the most useful parameter in the analysis of ancient wave events and deposits (cf. Nandasena et al., 2022). Moreover, only the wave height records of historical and modern tsunamis and typhoons are available for comparison in the study area.

The previously modified Nott equations, which consider the maximum lifting surface, shore slope angle, and transport modes of sliding, rolling, and saltation, and cover submerged, subaerial, and joint-bounded scenarios were adopted in the calculation (Table 2; Nott, 2003; Pignatelli et al., 2009; Barbano et al., 2010; Lorang, 2011; Nandasena et al., 2022). The modifications also incorporate the virtual boulder shape, volume, and projected surfaces into the drag and lift coefficients (Table 2; Nandasena et al., 2022). The Hudson formula is then adopted for independent storm wave estimates of the beach–intertidal zone (Lorang, 2011; Hudson, 1953). The Froude Number is set at 2.0 for tsunami waves and 1.0 for storm waves. The choice is based on the tendency of these waves to induce highly supercritical and critical flows, respectively (Nott, 2003). It is worth noting that various supercritical flow regimes are associated with both tsunami and storm waves (Cox et al., 2020; Nandasena, 2020), which will be addressed in Sect. 4.1. The wave periods are then derived from (1) the estimated heights, and

已删除: unit… hereafter referred to asdenoted…'Chungtun-1CTB (CT…boulder,'),…was selected for analysiscalculation…due tobecause…its significantly larger size compared to the other boulders … in the outcrop are significantly smaller …Fig. 3a). These cliff-top …oulder clasts form a clusterare …in a mud-matrix-supported by a …ravel layerand mud matrix…that form…s a …aterally continuous andgravel…graduallylayer (MECT-1)…thinthat pinch…es…out upward from 2.5 to 4.0 m a.s.l. This layer is referred to as 'Chungtun-1 layer' (Fig. 3a). Marine shells and rounded pumice pebbles that …are abundant in theboth…matrix and gravel layer,…and and are …lso found…on the channelmodern…beaches in the region…(Fig. 3b);…however, they areare…absent in the underlying basalt basement, …and basal soil,…as wellnd…as the overlying angular-gravel colluvium. Accordingly, it is assumed that the cliff-top boulder and gravel layer have a marine sediment origin for the cliff-top boulder and gravel layer is assumed ... [11]

已删除: The CTB m…trics of the Chungtun-1 boulder were measured using Autodesk Meshmixer and Context Capture; the measurements include:…a density of 2.91 g cm^{-3} density… a volume of 0.73 m^3 volume, a mass of 2.10–….15…t mass… an axis length og an axis length of ….71–0.69 m, and a projected surface area of a projected surface of ….66–1.01 m^2, were measured using Autodesk Meshmixer and Context Capture…(Fig. 3c). The boulder shapeCTB…is angular in shape…,…indicatinging…its origin from a joint-bounded source in the intertidal–subtidal zone sincebecause…subaerial spheroidal weathering and rock residue are well developed acrossll over…the islands, including the CT-1 …asalt cliff of outcrop Chungtun-1 (Fig. 3a). There is A…n intertidal rock exposure that is loc…ted…0.5 m below sea level, which exhibits …well-developed joint fractures and rock debris similar in size and shape to the comprises isolated and stacked …oulder clasts of the Chungtun-1 outcrops of sizes and shapes that are comparable to the CTB may be the source of the studied boulder…(Fig. 3 ... [12]

已删除: performed in …wo main proceduresparts… (1) an initial …stimation of the minimum wave heights and periods required for theo…initiatione…of transport of the CTB …hungtun-1 boulder using the modified incipient motion formulas, and (2) distinguishing between the typhoon and tsunami wave origins by comparing the estimationed…results with various wave sources such as modern and ancient records of waves associated with…tsunami waves, typhoon waves, and the …00 …year significant waves, and 100-year surge (Cox et al., 2020) heights… The C…omparisonng…alsoestimation with records…integrates the constraints fromassociated with…the geomorphology, bathymetry, ancient local sea level, and the ratio of wave height to water depth at the wave break (Cox et al., 202 ... [13]

已删除: that…consideruse…the maximum lifting surface, shore slope angle, and transport modes of sliding, rolling, and saltation, into account …nd cover submerged, subaerial, and joint-bounded were adopted in the initial…calculation (Table 2; Nott, 2003; Pignatelli et al., 2009; Barbano et al., 2010; Lorang, 2011; Nandasena et al., 2022). The modifications also incorporate the virtual boulder shape, volume, and projected surfaces into the drag and lift coefficients (Table 2; Nandasena et al., 2022). The Hudson formula is then adopted for independent storm wave estimates of the beach–intertidal zone (Lorang, 2011; Hudson, 1953). The Froude Number is set at 2.0 for tsunami waves and 1.0 for storm waves. The choice is based on the tendency of these waves to induce highly supercritical and critical flowsA ratio of 0.25 was obtained for tsunami and storm wave heights using 1.0 and 2.0 as Froude Numbers to describe the storm and tsunami waves ... [14]

(2) the modified Noortmets equation for maximum water flooding (Noormets et al., 2004; Barbano et al., 2010; Lorang, 2011). In the Noortmets equation, the cliff-top elevation is measured at the outcrop, 2.5 m a.s.l., and the minimum run-up height is marked by the pinch-out of Chungtun-1 layer at 4.0 m a.s.l. (Fig. 3a). The regional bathymetric gradient, which is used to delineate the ratio of wave height to water depth at the wave break, was derived from the XX' transect between the Chungtun Channel and an abandoned offshore buoy in the northeast (Fig. 1b, Table 2; Collins, 1970; Noormets et al., 2004). The water depth change is 20 m, the distance is 8,380 m, and the ratio is 0.73.

已删除: For
已删除: wa
已删除: wa
已删除: MECT-1
已删除: in the second part of the approach
已删除: CT channel
已删除: NE

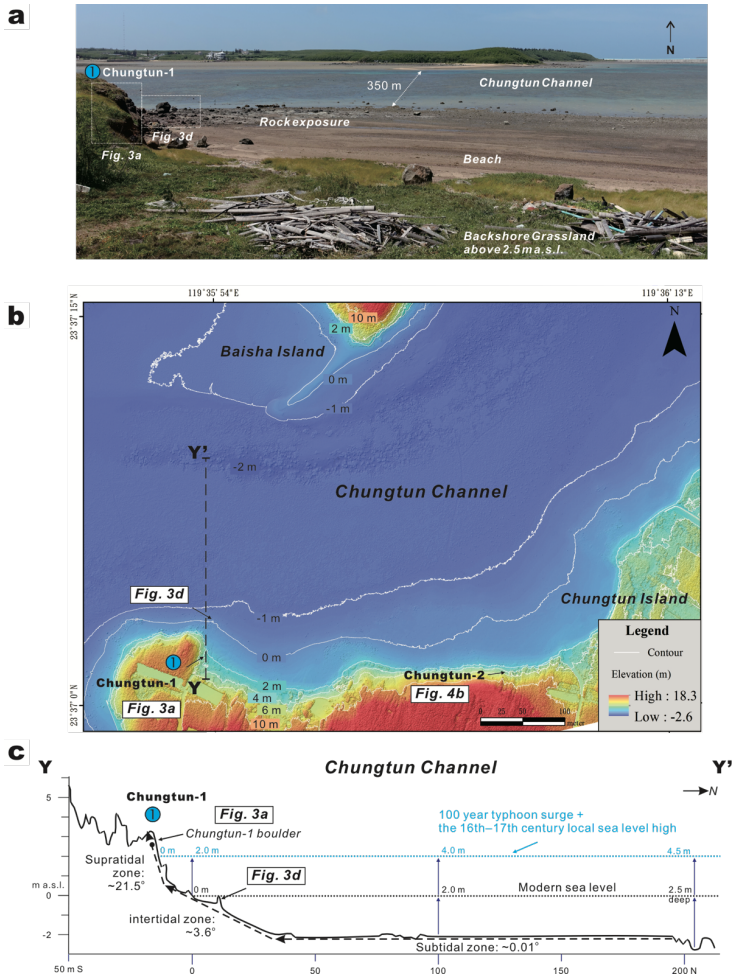

685 **Figure 2: Regional view and bathymetry of the outcrop Chungtun-1. The location is shown in Fig. 1b (blue circle 1). (a) Chungtun Channel at low tide, the channel is less than 2.5 m in depth. (b) DEM image. (c) YY' transect showing the flat subtidal, the gentle intertidal, and the steep supratidal zones. The blue dotted line marks the maximum depth in the 17th century, when the local sea level was 0.2 m higher (Chen and Liu, 1996) and superimposed by the 100-year typhoon surge at 1.8 m a.s.l.**

已删除: T
已删除: L
已删除: illustrated
已删除: CT-1 shore and interisland CT Channel
已删除: .
已删除: C
已删除: ,
已删除: and
已删除: an increase in the slope angle from
已删除: to
已删除: in the transect
已删除: estimated
已删除: is
已删除: 100

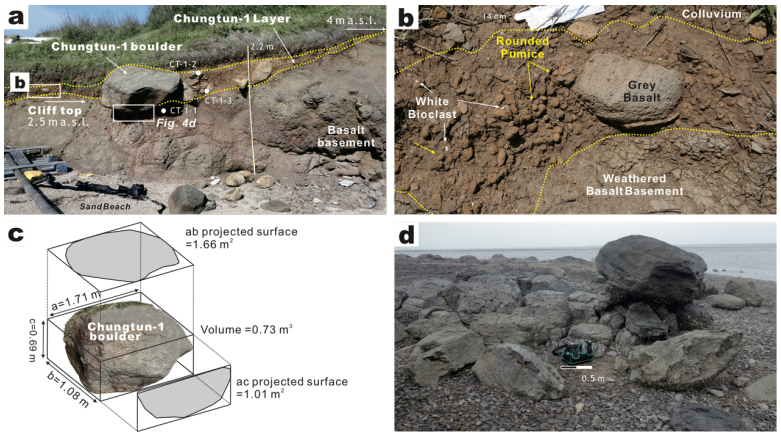

Figure 3: Outcrop views and scanned boulder image. Outcrop locations a and d are shown in Fig. 2. (a) Outcrop section from the basalt basement to the Chungtun-1 layer and topsoil. A boulder cluster, including the Chungtun-1 boulder, is prominent in the matrix-supported Chungtun-1 layer that pinches out upward from 2.5 to 4.0 m a.s.l. Note the spheroidal weathering and rock residues in the basement. CT-1-1–3 marks the radiocarbon sample locations. (b) Close-up view of the matrix-supported Chungtun-1 layer composed of rounded brownish pumice, grey basalt, and white bioclast. (c) Chungtun-1 boulder metrics obtained using Autodesk Meshmixer and Context Capture. (d) Intertidal joint-bounded basalt exposure, boulder stacks, and isolated boulders. Note that the boulders are comparable in size and shape to those in the Chungtun-1 layer in Fig. 3a.

Table 2. Modified incipient motion formulas adopted in this study.

Initial transport mode	Submerged	Subaerial	Joint bounded
Sliding*	$H \geq \frac{2C_{vv}\left(\frac{\rho_s}{\rho_w}-1\right)c(\mu_s\cos\theta+\sin\theta)}{Fr^2\left[C_{dv}\left(\frac{c}{b}\right)+\mu_s C_{lv}\right]}$		—
Rolling/overturning*	$H \geq \frac{2C_{vv}\left(\frac{\rho_s}{\rho_w}-1\right)c\left(\cos\theta+\frac{c}{b}\cdot\sin\theta\right)}{Fr^2\left[C_{dv}\left(\frac{c^2}{b^2}\right)+C_{lv}\right]}$		—
Saltation/lifting*	$H \geq \frac{2C_{vv}\left(\frac{\rho_s}{\rho_w}-1\right)c\cdot\cos\theta}{Fr^2 C_{lv}}$		$H \geq \frac{2C_{vv}\left(\frac{\rho_s}{\rho_w}-1\right)c(\cos\theta+\mu_s\sin\theta)}{Fr^2 C_{lv}}$
Hudson Formula**	$H=\left(\left(K_D\left(\frac{\rho_s-\rho_w}{\rho_w}\right)^3\cot\alpha\right)V\right)^{1/3}$		
Wave period I**	$P=\left(\frac{2}{g}\right)\cdot\left(\frac{\rho_w}{\rho_s-\rho_w}\right)\left(\frac{C_{dv}}{\tan\theta}\right)\left(\frac{h_{clast}}{b}\right)\sqrt{g\cdot(W_b+H_S)}$		

已删除: of the CTB, MECT-1 gravel, and exposed intertidal rock…
已删除: L
已删除: is
已删除: provided
已删除: CT-1
已删除: cliff
已删除: up
已删除: ME
已删除: T
已删除: Matrix-supported
已删除: s
已删除: CTB
已删除: are
已删除: ME
已删除: T
已删除: ME
已删除: T
已删除: that is
已删除: CTB
已删除: to the CTB
已删除: both

II***	$P = {5 \cdot X_{max}} / {\cos\delta \cdot \sqrt{g(R-E)}}$
Wave height/water depth ratio****	${H_S}/{W_b} = 0.72 + 5.6 \cdot \tan\beta$

* Nott (2003), Nandasena (2020), Nandasena et al. (2022); ** Lorang (2011); *** Barbano et al. (2010); **** Collins (1970).
Wave height: H; Storm wave weight: H_S; Wave period: P; Water depth at wave break: W_b.
Chungtun-1 boulder axis lengths: a = 1.71 m; b = 1.08 m; c = 0.69 m. Volume: V, 0.73 m^3. Projected ab surface: A_{ab}, 1.66 m^2; Projected ac surface: A_{ac}, 1.01 m^2. Density: ρ_s, 2910 kg m^{-3}; Seawater density: ρ_w, 1020 kg m^{-3}.
Virtual lift coefficient: $C_{lv} = \frac{A_{ab}}{ab} C_l$; Virtual drag coefficient: $C_{dv} = \frac{A_{ac}}{ac} C_d$; Virtual volume coefficient: $C_{vv} = \frac{V}{abc}$.
Lift coefficient: C_l, 0.178; Drag coefficient: C_d, 1.95; Static friction coefficient: μ_s, 0.7; K_D for smooth stone: 1.5; Froude number: Fr, 1 for storm wave, 2 for tsunami wave; Gravity: g, 9.8 m s^{-2}.
Shore slope: θ; Beach slope: α; Regional slope: β, 20/83800 (X-X' in Fig. 1b); Mean CT-1 coastal overland slope: δ, 21.5°.
Chungtun-1 boulder elevation: h_{clast}, 2.5 m a.s.l.; Maximum flooding distance from the probable intertidal source to Chungtun-1 outcrop: X_{max}, 31.7 m; Run-up of event layer: R, 4.0 m a.s.l.; Cliff top elevation: E, 2.5 m a.s.l.

3.2 Coastal outcrops and facies-stratigraphic analysis

To obtain a better understanding of the facies and stratigraphic constraints on the transport and deposition of the cliff-top boulder, the Chungtun-1 outcrop and three additional outcrops with gravel layers of marine sediment origin were investigated; these include the adjacent outcrop Chungtun-2 (Figs. 2b and 4a) and the Watong and Shetoushan outcrops located at a distance (blue circles 2 and 3 in Fig. 1b; Fig. 4b–c). A previously reported outcrop at Suogang was included for comparison (blue circle 4 in Fig. 1b; Lu et al., 2019). All studied outcrops are situated in the supratidal zone with top surfaces at elevations of 2.5–5.3 m a.s.l.

Analyses of the sedimentary facies, granulometry, and radiocarbon dating were conducted on the newly investigated outcrops. Facies analysis involves the integration of lithology, sedimentary structure, and fossil content. Granulometric samples were collected from the Chungtun-2 and Shetoushan outcrops, chosen for their substantial total thicknesses and massive gravel layer texture. These samples were analyzed using a sieve shaker and a Microtrac S3500 laser particle size analyzer. Charred material samples from the investigated gravel layers and ambient deposits were sent to Beta Analytic, Miami, Florida, USA, for radiocarbon dating. The modeled ages of the newly investigated and previously-reported gravel layers were calculated using OxCal 4.4 from the University of Oxford and the IntCal13 calibration curves (Ramsey, 2021; Reimer et al., 2013).

格式化: 行距: 單行間距
已刪除: CTB
已刪除: CTB
已刪除: v
已刪除: CTB
已刪除: d
已刪除: CTB
已刪除: CT-1
已刪除: better
已刪除: the
已刪除: CTB
已刪除: T
已刪除: supratidal
已刪除: that were deposited during a marine event
已刪除: T
已刪除: two distant outcrops
已刪除: T
已刪除: TS
已刪除: Suogang/
已刪除: G outcrop
已刪除: an
已刪除: applied
已刪除: t
已刪除: (CT-1, 2, WT, and STS)
已刪除: es
已刪除: with
已刪除: sections
已刪除: T
已刪除: TS
已刪除: characterized
已刪除: by
已刪除: large
已刪除: marine
已刪除: ,
已刪除: and
已刪除: marine
已刪除: both
已刪除: marine

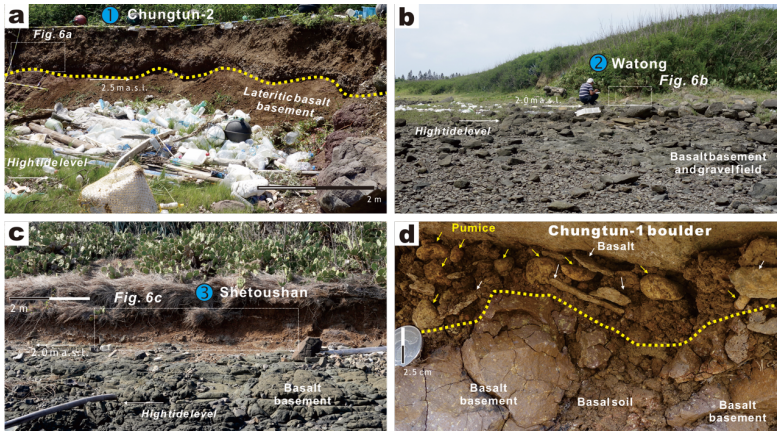

Figure 4: Regional and close-up views of the investigated outcrops at low tide. (a) Chungtun-2 outcrop with the basalt basement top at 2.5 m a.s.l. (location in Fig. 2b). (b) Watong outcrop with the basalt basement top at 2.0 m a.s.l. (location in Fig. 1b). (c) Shetoushan outcrop with the basalt basement top at 2.0 m a.s.l. (location in Fig. 1b). (d) Close-up view of the base of the Chungtun-1 boulder. Location is shown in Fig. 3a. The base is separated by the mud-supported gravels from the basalt basement and basal soil. The gravels include rounded pumice (yellow arrows) and platy–angular basalt (white arrows).

4 Results

4.1 Wave conditions during cliff-top boulder transport and deposition

4.1.1 Storm wave height

The estimated minimum storm wave height required to initiate the transport of Chungtun-1 boulder is 0.87–9.5 m (Table 3), which is well within the 6.8–17.8 m maximum height of modern typhoon waves and the previously estimated significant wave heights for the 50- and 100-year periods (Table 1; Central Weather Bureau, 2022). These results seem plausible because western Pacific typhoons are notoriously powerful, and the Chungtun-1 boulder is relatively small in volume and mass.

However, when considering the ancient bathymetry during deposition, facies, and probable transport modes, typhoon waves are unlikely to have been responsible for the deposition of Chungtun-1 boulder at its current cliff-top position. According to the dating results, Chungtun-1 boulder may have been deposited in the 16th–17th centuries (CT-1-1 and 3 in Fig. 3a and Table 4). During this period, the maximum water depth in the Chungtun Channel could have reached 4.5 m because the local sea level was approximately 0.2 m higher than it is at present, allowing a 100-year surge of 1.8 m a.s.l. to occur (Fig. 2c; Chen and Liu, 1996; Central Weather Bureau, 2022). The tallest typhoon waves that can form in the subtidal–intertidal water depths

已删除: **Holocene …utcropsection… at low tide. (a) ChungtunT…2 outcropsection…withlying above…the basalt basementplatform…top at 2.5 m a.s.l. (location in Fig. 2b). (b) WatongT…outcropsection…lying above…ith the basalt basementplatform…top at 2.0 m a.s.l. (location in Fig. 1b). (c) ShetoushanTS…outcropsection…with the basalt basementplatform…top at 2.0 m a.s.l. (location in Fig. 1b). (d) Close-up view of the base of the Chungtun-1 boulder. Mud and gravel matrix beneath the CTB in MECT-1 layer (l…ocation is shown in Fig. 3a)… The base is separated by the mud-supported gravels from the basalt basement and basal soil. The gravel component… includes** ... [15]

已删除: **CTB**

已删除: **W**

已删除: CTB…transport of Chungtun-1 boulder of…is 1.22….87–9.5 m (Table 3), which is well within the 6.8–17.8 m maximum height ofobserved…for …odern typhoon waves and the previously estimateds of the…significant wave heights for the 50- and 100-year periods (Table 1; Central Weather Bureau, 2022). These results seem plausible because western Pacific typhoons are notoriously powerful, and the the …hungtun-1 boulderCTB ... [16]

已删除: taking…the ancient bathymetry during deposition, facies, and probable transport modes into account… renders …yphoon waves are unlikelysuitable…tocandidates…havefor…been responsible for the deposition of Chungtun-1 boulderCTB…at its current cliff-top position. According to the dating results, the …hungtun-1 boulderCTB…maywas…haveprobably…been deposited in the 16th–17th centuries (CT-1-1 and 3 in Fig. 3a and Table 4). During this period, the maximum water depth in the CT Channel…hungtun Channel could have reachedincrease from 2.5 to…4.5 m because the local sea level was approximately 0.2 m higher than it is at present, allowing a 100 ... [17]

(1.46–3.29 m; wave height = 0.73 × water depth) can trigger the sliding and rolling of the Chungtun-1 boulder upon breaking (Table 3). The sliding–rolling movement is likely to cease in the steeper supratidal zone because the estimated minimum waves are too tall to form in the shallow depth of the inundated supratidal zone and will break earlier before attenuating rapidly and exponentially landwards (Barbano et al., 2010; Goto et al., 2009). The estimated minimum wave heights of 8.5–9.5 m required for saltation and lift from the probable intertidal joint-bounded source cannot occur in the 4.5-m deep Chungtun Channel.

The onshore flows induced by storm waves have been determined as supercritical, with a Froude Number greater than 1, and capable of displacing large coastal cliff-top boulders (Cox et al., 2020). In the case of the Chungtun-1 boulder, which stands at a height of 0.69 m, the estimated Froude Number is between 1.0 and 1.6 for the flow to be able to overtop and entrain the boulder into motion (cf. Nandasena, 2020), and the estimated minimum wave height is 1.1–1.9 m. Accordingly, the corresponding water depth required is 1.46–2.65 m, which generally exceeds the depth of the inundated supratidal zone of the 17th century (<2.0 m). Alternatively, the estimated waves will break and attenuate in the deeper channel, and the boulder will stop moving in the intertidal–supratidal zone.

4.1.2 Tsunami wave height

The estimated minimum heights of tsunami waves fall in two groups: (1) heights ranging from 0.22–0.51 m, which are associated with the initiation of Chungtun-1 boulder sliding and rolling, and are comparable to the 0.4 m high tsunami that inundated the Penghu Islands in 1994, (2) The second group consists of heights ranging from 2.13–2.38 m, linked to the saltation and joint-bounded scenario (Table. 3). The first group must be modified to >0.69 m or 0.87–2.03 m. It is because the initial estimate is smaller than the 0.69 m boulder height, which is discordant with the formula assumption (cf. Nandasena, 2020). This suggests that the supercritical waves (Froude Number = 2) are at least taller than the boulder height, or the waves are less supercritical (1< Froude Number <1.6) and may be as tall as the estimated storm waves (0.87–2.03 m high, Table 3). As for the second group, the minimum height of the supercritical waves (Froude Number = 2) is concordant with the boulder height assumption. Alternatively, the wave height may range between 3.33–3.72 m and 9.16–9.50 m as the flow regime becomes less supercritical (1< Froude Number <1.6).

Based on the facies and outcrop geomorphology, it appears that these tsunami wave height minima are largely insufficient to deposit the Chungtun-1 boulder on the cliff top. The boulder is underlain by the pumice-bearing gravel and mud matrix above the cliff basement (Fig. 4d) and evidently part of the matrix-supported Chungtun-1 gravel layer (Fig. 3a–b). This indicates that the terminal boulder transport to the cliff top was controlled by suspension-rich turbulent flow process and very likely involved rolling or saltation before deposition. This finding is in agreement with the bore-like long-wave-length waves that tend to lead to boulder rolling and saltation (Imamura et al., 2008), especially for boulders smaller than 2 m in length, such as the Chungtun-1 boulder (Nandasena et al., 2011). The greater height of the first/sliding–rolling group, 1.65–2.03 m, is sufficient to rotate the median point of the 1.7-m long boulder to exceed the cliff top elevation (2.50 = 1.65 + 1.7/2), enabling the cliff-top deposition (Fig. 3a). The smaller height range of 0.69–1.65 m would cause the boulder to rotate and reach below

已刪除: ,…can triggerinitiate…the sliding and rolling of the the …hungtun-1 boulderCTB…upon breaking (Table 3). Theis…sliding–rolling movement is likely to cease in the steeper supratidal zone because the estimated minimum waves are too tall to form in the shallow depths…of the inundated supratidal zone and will break earlier before attenuating rapidly and exponentially landwards (Barbano et al., 2010; Goto et al., 2009). The estimated minimum wave heights of 8.5–9.5 m that would be …equired for saltation and lift from the probable intertidal joint-bounded source cannot occur in the 4.5 …-m deep ChungtunT ... [18]

格式化: 縮排: 第一行: 0.65 公分

已刪除:

已刪除: the …sunami waves fall in two groups: (1) heights ranging from 0.33…2–0.51 m, which are associated with thefor…initiation of Chungtun-1 boulder sliding and–…rolling, which …nd areis…comparable to the 0.4 m high tsunami that inundated the Penghu Islands in 1994, … and …2) The second group consists of heights ranging from 2.13–2.38 m, linked tf…r ... [19]

格式化: 縮排: 第一行: 0.65 公分, 格線被設定時，自動調整右側縮排, 調整中/英文字之間的空白, 調整中文/數字之間的空白

已刪除: ... [20]

the cliff top elevation and finally rest on the cliff slope. However, given the tallest wave height of 2.03 m, the finer sediment would be trapped below the cliff top, resulting in a clast-supported fabric rather than the observed matrix-supported fabric (Figs. 3a and 4d).

The wave height of the second/saltation and joint-bounded group is sufficient to lift the 1.7-m long Chungtun-1 boulder onto the cliff top, while the 2.13–2.38 m tall waves of the supercritical regime (Froude Number = 2) may lead to the deposition of fine-grained material below the cliff top and the formation of an undetected clast-supported fabric. Furthermore, additional overtop wave run-up and sediment transport are required to prevent the boulder from falling back down the cliff due to tsunami backwash (Pignatelli et al., 2009; Imamura et al., 2008; Lorang, 2011). Considering that the Chungtun-1 boulder was probably moving in a rolling–saltation manner before deposition, the substantial depth required for the cliff-top run-up/overflow is unlikely to result from tsunami waves that are only 2.13–2.38 m in height (Figs. 3a and 4d).

Taken together, these results suggest that a tsunami wave height significantly exceeding majority of the calculated results is required. It is estimated to be 3.19 m, ensuring that the cliff-top overflows surpasses the 0.69-m tall boulder, as well as allowing the terminal rolling before deposition. Alternatively, the tsunami waves were low in the supercritical regime (1< Froude Number <1.6) and at least taller than 3.37 m (2.5 m cliff height + 0.87 m rolling wave height). The outcrop observation also indicates the run-up and local wave height could 4.0 m, based on the pinch-out of the Chungtun-1 layer at 4.0 m a.s.l. (Fig. 3a; Pignatelli et al., 2009; Nanayama and Shigeno, 2006; Paris et al., 2018).

4.1.3 Wave period

The estimated wave period ranges from 2.9–15.0 s in the supratidal zone to 19.6–132.9 s in the intertidal zone and 6.47×10^{3}–3.55×10^{4} s in the subtidal zone (Table 3). According to the formulas used (Table 2), the prominent seaward increase is primarily influenced by the slope angle, which decreases drastically to 0.01° in the nearly horizontal subtidal zone (Fig. 2; Barbano et al., 2010; Lorang, 2011). The observed increases in water depth and wave height also favor a wave period increase.

Comparing the estimated wave periods with the modern wave records, it is evident that typhoon waves play an insignificant role in the transport and deposition of the Chungtun-1 boulder (Tables 1 and 3). Only the estimated range of 6.8–15.0 s for the supratidal zone is comparable to the modern wave maximum of 8.7–23.2 s, which, however, occurs at a depth of 20–40 m offshore (Central Weather Bureau, 2022).

In contrast, the estimated subtidal period that is associated with the minimum tsunami wave height and ranges from 1.5–4.9 h (5.47×10^{3}–1.77×10^{4} s) is comparable to the typical periods of modern tsunamis (Barbano et al., 2010; Lorang, 2011). The estimated period extends to 5.8 h when the waves are 3.19 m high. The successive shortening of the estimated period in the intertidal–supratidal zone likely corresponds to the deceleration of the tsunami waves through shoaling, which also causes a landward decrease in wavelength and a landward increase in wave height. Therefore, the Chungtun-1 boulder transport is attributed to long-periodicity tsunami or tsunami-like composite waves produced by the interplay between typhoon waves,

已删除: The 0.44–0.51 m high tsunami waves that would be required to initiate rolling of the CTB would cause it to rotate and reach 2.14–2.21 m a.s.l., before finally depositing it on the slope of the 2.5-m-high cliff (Fig. 3a). The tsunami waves need to be 0.8 m high to rotate the CTB to reach the cliff top elevation and to be over 1.65 m high (0.8 + 1.7/2) to rotate the CTB median point onto the cliff top… However, given the tallest wave height of 2.03 m, theIn the sliding–rolling transport, any…accompanying coeval …iner sediment would be trapped below the cliff top, would be deposited separately below ... [21]

已删除: minimum tsunami…wave height of the second/saltation and joint-bounded scenarios, 2.13–2.38 m…group,…is sufficient to lift the 1.7 …-m long Chungtun-1 boulderCTB to 3.83–4.09 m a.s.l.…onto the cliff top, while the 2.13–2.38 m tall waves of the supercritical regime (Froude Number = 2) may while…lead to the deposition of fine-grained materialdepositing…the coeval finer sediment …elowon…the cliff slope below…top and the formation of an undetected clast-supported fabric. Furthermore,However,…additionalfurther …overtop wave run-up sediment transport are required to prevent the boulderCTB…from falling back down the cliff dueas…toa result of…tsunami backwash (Pignatelli et al., 2009; Imamura et al., 2008; Lorang, 2011). Considering that Since …he the terminal CTB ... [22]

已删除: Collectively… these results suggest that a tsunami wave height significantly exceeding majority of the calculated results is required. It is estimated to beof…3.0 …9 m, would be required…to …nsuringmaintain…that the cliff-top overtop …lows surpassesat…the 0.69estimated …minimum…tallheight of…boulder,0.51 m…as well as allowingfor …the terminal rolling beforeCTB…deposition on the 2.5 m high cliff top… Alternatively, the tsunami waves were low in the supercritical regime (1< Froude Number <1.6) and at least taller than 3.37 m (2.5 m cliff height + 0.87 m rolling wave height). The outcrop observation also indicatesIn addition, the MECT-1 pinch-out at 4.0 m a.s.l. marks…the minimum …un-up and local wave height couldat ... [23]

已删除: 2

已删除: 3.4….9–15.0 s in the supratidal zone to 19.6–132.9 s in the intertidal zone and 6.47×10^{3}–3.55×10^{4} s in the subtidal zone (Table 3). According to the formulae… used (Table 2), the prominent seaward increase is primarily influencedcontrolled…by the slope angle, which decreases drastically to 0.01°° ... [24]

已删除: ed to the wave records from Taiwan,…thate…typhoon waves play appear …n insignificantrrelevant…role in the transport deposition of the Chungtun-1 boulderrms of the estimated wave period…(Tables 1 and 3). Only the estimated range of 6.8–15.0 s that was obtained …or the supratidal zone is comparable to the modern wave maximum of 8.7–23.2 s, which, however, occurs offshore …t a depth of depths of ... [25]

已删除: of…1.8…–4.9 h (6….47×10^{3}–1.77×10^{4} s) is comparable towithin…the range …ypical periods of modern tsunamis (Barbano al., 2010; Lorang, 2011). The estimated period extends to 5.6 … h when the waves are 3.0 …9 m high, allowing waves to overflow the 2.5 m high cliff top and maintain the minimum 0.5 m depth… The successive shortening of the estimated period in the intertidal–supratidal zone likelyprobably…corresponds to the shoaling that is due to…deceleration of the tsunami waves through shoaling, which alsond…also …auses a landward decrease in wavelength andlongside…a landward increase in the…wave height. Therefore, the Chungtun-1 boulderCTB…transport is inferred to be…attributed toassociated with ... [26]

surge, infra-gravity waves, and astronomical high tides (Baumann et al., 2017; Brill et al., 2016; Nakamura et al., 2014; Sohn and Sohn, 2019; Watanabe et al., 2017).

Table 3. Results of wave estimation from equations in Table 2.

Wd†, θ		**Supratidal 2.0 m>Wd, 21.5°**	**Intertidal 2.0<Wd<4.0 m, 3.6°**	**Subtidal 4.0<Wd<4.5 m, 0.01°**
Sliding	H_S, P_S, W_b	1.27, 5.8, 1.6	0.94, 33.2, 1.3	0.87, 1.09×10^4, 1.2
	H_T, P_T	0.32, 2.9	0.24, 16.6	0.22, 5.47×10^3
Overturning/ Rolling	H_S, P_S, W_b	2.03, 7.3, 2.8	1.80, 45.6, 2.5	1.74, 1.55×10^4, 2.4
	H_T, P_T	0.51, 3.6	0.45, 22.9	0.44, 7.73×10^3
Saltation	H_S, P_S, W_b	8.50, 15.0, 11.6	9.14, 103.2, 12.5	9.16, 3.55×10^4, 12.5
	H_T, P_T	2.13, 8.5	2.28, 52.7	2.29, 1.77×10^4
Joint bounded	H_S, P_S, W_b		9.50, 132.9, 13.0	
	H_T, P_T		2.38, 52.7	
Hudson F.	H_S, P_S, W_b		4.88, 95.1, 6.68	
Ps/Noormets Eq.	44.4s			

†: maximum water depth during the 100 year surge in the 17th century; θ: shore slope.

H_S: storm wave weight (m); P_S: storm wave period (s); W_b: wave break depth (m), i.e., $H_S\,0.73^{-1}$.

H_T: tsunami wave weight, i.e., $0.25 \cdot H_S$ (m); P_T: tsunami wave period (s).

Table 4. AMS Radiocarbon dating results. See sample locations in Figs. 3a and 5a–b.

Sample No.	Anal. No.	Material	$\delta^{13}C$ (‰)	Conventional age	2 Sigma calibration
CT-1-1	528841	Charred material	−13.5	280 ± 30 BP	Cal 1500 to 1658 CE
CT-1-3	539055	Charred material	−16.1	250 ± 30 BP	Cal 1510 to 1667 CE
CT-1-2	528843	Charred material	−17.1	105.76 ± 0.39 pMC	Cal 1957 to 2009 CE
CT-2-1	539056	Charred material	−16.8	540 ± 30 BP	Cal 1326 to 1439 CE
CT-2-2	538845	Charred material	−18.0	450 ± 30 BP	Cal 1418 to 1474 CE

已删除: ↵
已删除: 78
已删除: 6.8
已删除: 2.4
已删除: 1.32
已删除: 39
已删除: 1.8
已删除: 1.22
已删除: 29
已删除: 8
已删除: 44
已删除: 3.4
已删除: 33
已删除: 19
已删除: 33
已删除: 6
已删除: locations
格式化: 靠左

WT-1	563788	Charred material	−13.5	420 ± 30 BP	Cal 1455 to 1625 CE
WT-2	563789	Charred material	−17.0	200 ± 30 BP	Cal 1645 to 1948 CE
STS-E-1-2	510514	Charred material	−12.4	110 ± 30 BP	Cal 1681 to 1939 CE
STS-E-2	484573	Charred material	−12.2	320 ± 30 BP	Cal 1487 to 1640 CE
STS-E-3	484574	Charred material	−13.0	350 ± 30 BP	Cal 1479 to 1630 CE
STS-E-4	484575	Charred material	−12.9	390 ± 30 BP	Cal 1437 to 1506 CE
SG-3‡	435211	Charred material	−14.6	890 ± 30 BP	Cal 1040 to 1220 CE
SG-2‡	405582	Foraminifers	+0.2	960 ± 30 BP	Cal 1030 to 1230 CE
SG-4‡	405583	Charred material	−13.7	650 ± 30 BP	Cal 1291 to 1403 CE
SG-5‡	438347	Charred material	−15.7	100.6 ± 0.3 pMC	post 1950 CE

‡ Lu et al. (2019).

4.2 Supratidal Upper Holocene facies

已刪除: ↵

4.2.1 Description

The newly investigated and previously-reported Upper Holocene outcrops are situated on the supratidal shore platforms at evevations of 2.5 m a.s.l. (Chungtun-1 and 2; Figs. 3a and 4a) and 2.0 m a.s.l. (Shetoushan, Watong, and Suogang; Fig. 4a–c). The outcrops have a thickness ranging from 0.4 to 1.2 m and are primarily composed of common colluvium and dune deposits on the islands (Fig. 5a–b; Yen and Lee, 2018; Lu et al., 2019). Overlying the weathered, lateritic basalt basement, the Upper Holocene is composed of the mottled/weathered gravelly colluvium (Chungtun-1 and 2 outcrops; Figs. 3b and 6a), bioclastic sand (Watong outcrop; Fig. 6b), and brownish sandy soil (Shetoushan and Suogang outcrops; Fig. 6c–d) as well as the top humic soil. The mottled brownish sandy soil and colluvium are poorly sorted (CT-2-03, STS-01, 03, 04, and 06 in Fig. 5c) and contain angular basalt debris (Figs. 3a–b, 4d, 6a, c–d). The bioclastic sands are better sorted and predominantly consist of shell fragments and foraminifers, forming local dunes (Figs. 4b and 6b). According to the radiocarbon dating results, the newly-studied sections have accumulated since the 15th century, and the Suogang section started accumulating in the 10th century (Fig. 5a–b, Table 4; Lu et al., 2019).

Embedded in the colluvium and dune deposit, the candidate gravel layers that are associated with events of marine inundation and deposition are 10–70 cm thick and lie at an elevation of 2.0–4.5 m a.s.l. (Fig. 5a–b). These layers are poorly sorted, matrix-supported, massive/structureless, and in sharp basal contact with the weathered basalt residues and mottled deposits (Figs. 3b and 6). In addition to field observation, the sharp contact is also evidenced by abrupt upward increases in granulometry from the lateritic basalt basement to the CT-2-01 sample, from STS-01 to 02, and from STS-04 to 05 (Fig. 5b–

已刪除: ly-…and previously-reportest…udied…Upper Holocene outcrops are situated at…np…the supratidal shore platforms at evevations of 2.5 m a.s.l. (ChungtunT…1 and 2; Figs. 3a and 4a) and 2.0 m a.s.l. (ShetoushanTS… WatongT… and SuogangG… Fig. 4a–c). The outcrops have a thickness….rangingThe Upper Holocene deposits are…from 0.4 to–…1.2 m thick,…andmainly…arecomposed…primarily composed ofof…common colluvium,…and form …une deposits on the islands (Fig. 5a–b; Yen and Lee, 2018; Lu et al., 2019). Overlying the weathered, lateritic basalt basement, the Upper Holocene is composed of the mottled/weathered gravelly colluvium (ChungtunT…1 and 2 outcropsection…; Figs. 3b and 6a), bioclastic sand (WatongT…outcropsection… Fig. 6b), and brownish sandy soil (ShetoushanTS…and SuogangG…outcrops; Fig. 6c–d) as well asnd…the top humic soil. The mottled brownish sandy soil and colluvium are poorly sorted (CT-2-03, STS-01, 03, 04, and 06 in Fig. 5c) and contain angular basalt debris (Figs. 3a–b, 4d, 6a, c–d). The bioclastic sands are better sorted and predominanted…y cons… [27]

已刪除: while…thesection…SuogangG…section started to …ccumulatinge… [28]

已設定格式: 上標

已刪除: T…e candidate gravel layers that are associated with a …vents ofsupratidal…marine inundation and depositionevent (ME)…are 10–70 cm thick and lie at an elevation of 2.0–4.5 m a.s.l. (MECT-1 and other ME layers in …ig. 5a–b). The …eME…layers are poorly sorted, matrix-supported, massive/structureless, and in sharp basal contact with the weathered basalt residues and mottled deposits (Figs. 3b and 6). In addition to field observation, T … [29]

c). The gravel component includes basalt, pumice, and bioclast (Figs. 3a and 6; Fig. 5b; Lu et al., 2019). The basalt grain size is pebble–cobble in most of the examined candidate layers and reaches medium boulder in the Chungtun-1 layer (Fig. 3a). The pumice is rounded to subrounded in shape, pebble sized, and rusty–yellowish brown in color (Figs. 3b and 6a–b). The bioclasts include coral, mollusks, and foraminifera, and are characterized by articulated bivalves and well-preserved gastropods in the Shetoushan and Watong candidate layers (Fig. 6b and d). The matrix contains sediments that are similar to the underlying deposits and basement soils, including weathered–lateritic angular basalt debris, mottled brownish sandy soil, and bioclastic sand (Figs. 4d, and 6).

已删除: positions
已删除: , with the bioclast dominating in the MEWT, MESTS-a, and b layers
已删除: , increasing
已删除: to
已删除: small–
已删除: s
已删除: outcrop
已删除: T
已删除: MEWT,
已删除: ME
已删除: TS-a, and b
已删除: and
已删除: es

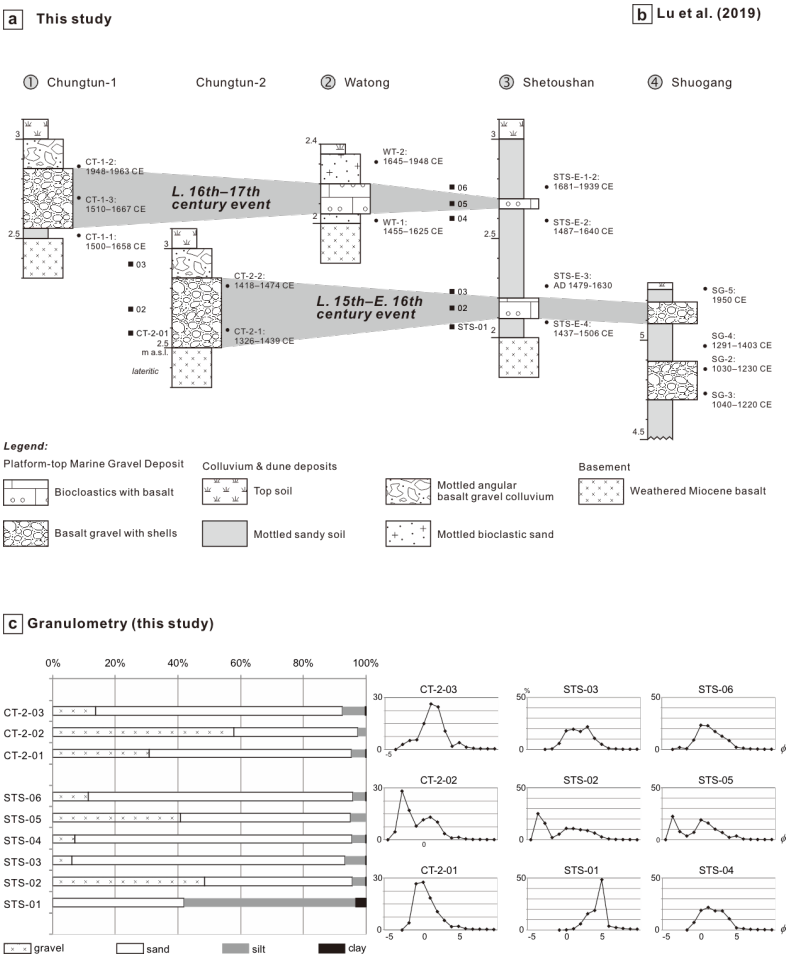

Figure 5: Stratigraphic correlation between outcrops and granulometry in this study. (a, b) Stratigraphic columns and correlation. Radiocarbon dating details are shown in Table 4. (c) Granulometry of Shetoushan and Watong outcrops showing an abrupt grainsize increase from the underlying samples to the candidate event layer samples (CT-2-01 and 02, STS-02 and 05).

已删除: can be found
已删除: the
已删除: TS
已删除: T
已删除: ME deposit

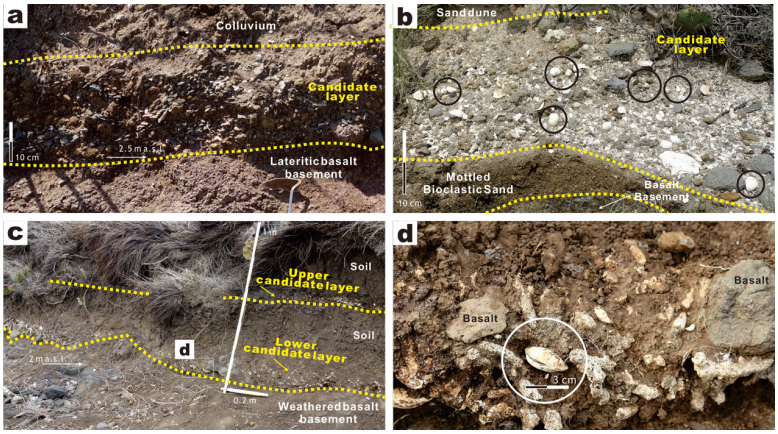

Figure 6: Outcrop views of the candidate event gravel layers in this study. See locations in Fig. 4. (a) Matrix-supported candidate gravel layer in the Chungtun-2 outcrop, characterized by pebbles of rounded rusty brown pumice, grey basalt, and white bioclast. (b) Candidate gravel layer in the Watong outcrop, characterized by well-preserved gastropods (black circles) and dominated by white bioclast with grey basalt and yellowish–rusty grey rounded pumice. (c) The Shetoushan outcrop showing intercalated soil and two candidate layers. (d) Close-up view of articulated bivalves (white circle) among the coral and basalt debris in the matrix-supported lower candidate layer in Fig. 6c.

4.2.2 Interpretation

The mottled colluvium and dune deposits are interpreted as terrestrial and/or supratidal accumulations that have been subjected to post-depositional soil formation. The soil preservation is attributed to the regional tectonic and geomorphological stability and the lack of wave and tidal reworking in the supratidal zone (Fig. 4a–c). The angular basalt colluvium in the Chungtun-1 and 2 outcrops may represent the deposits resulting from rockslides on relatively steep slopes (Figs. 2b and 4a). The mottled sandy soil in the Shetoushan and Suogang outcrops, as well as the bioclastic sand in the Watong outcrop, are likely indicative of supratidal dune deposits (Fig. 4b–c).

The matrix-supported candidate gravel layers, characterized by a sharp base and poor sorting, are interpreted as event deposits that record initial scouring and rapid fallout from suspension-rich turbulent flows (Fujiwara and Kamataki, 2008; Lowe, 1982; Nanayama and Shigeno, 2006; Paris et al., 2018; Madeira et al., 2020; Pérez-Torrado et al., 2006). Based on the coarse-grained size of cobble–boulder and the 1.7 m long Chungtun-1 boulder, the flow velocity, density, and turbulence were evidently high, creating a powerful combined hydraulic lift and dispersive pressure that effectively prevented settling during transport. During deposition, the rapid fallouts are highlighted by the matrix-supported gravel fabric and the mixed particles

已刪除: **marine**
已刪除: **ME**
已刪除: **T**
已刪除: **layer**
已刪除: **MEWT**
已刪除: **TS**
已刪除: **section**
已刪除: **marine event gravel (MESTS-a and b)**
已刪除: **ME**
已刪除: **STS-b**
已刪除: T
已刪除: appears to
已刪除: be
已刪除: result of
已刪除: rockslide
已刪除: the
已刪除: (
已刪除: TS
已刪除: G
已刪除:)
已刪除: nd
已刪除: (
已刪除: T
已刪除:)
已刪除: a
已刪除: like
已刪除: to be
已刪除: sharp-based, poorly sorted,
已刪除: s
已刪除: CTB
已刪除: ; thus,
已刪除: the
已刪除: could
已刪除: T

with a wide range of densities and sizes, including vesicular pumice, carbonate bioclast, and mafic igneous basalt (CT-2-01, 02, STS-02, and 05 in Fig. 5c).

The sediments found in the candidate gravel layers originated from coastal marine environments and were reworked from beach–dune environments to high supratidal location. The beach-derived sediments include bioclasts, such as coral, foraminifera, and mollusk, as well as pumice, all of which are commonly observed on local beaches (Figs. 3a and 4a–c). On the Penghu Islands, modern beach pumice includes stranded rafts from the 2021 submarine eruption in the southern Izu-Bonin Arc, whereas pumice is absent in the Miocene basalt and sedimentary basement (Yen and Lee, 2017. (in Chinese with English abstract); Yu et al., 2022). Ancient stranded pumice rafts are commonly incorporated into backshore event redepositions and have been reported in northern Taiwan from the past 2.4 ka (Yu et al., 2022). The redeposited dune and supratidal material is represented by angular basalt, brownish soil, and bioclastic sand in the matrix and is present in the sections below the candidate layers (Figs. 4d and 6a–d).

4.3 Age dating and correlation

The investigated Upper Holocene stratigraphy is best manifested by Shetoushan outcrop because of the continuous exposure with two candidate layers and the radiocarbon dates in ascending and decreasing order (Fig. 5a–b).

The lower Shetoushan layer is intercalated into sandy soil dating from the 15th–early 17th centuries. Laterally, the layer is comparable in age to the candidate layer in outcrop Chungtun-2 which was deposited in the 14th–15th centuries at the earliest based on the age of the detrital sediment matrix. The upper Suogang layer is also in a comparable age, overlying soil from the 13th–14th centuries.

The upper Shetoushan layer overlies the soil dating the 16th–17th centuries and underlies the soil dating the 17th–19th centuries; it is correlated with the Chungtun-1 layer and the calculated boulder, which were deposited in the 16th–17th centuries, according to the dating results obtained for the Chungtun-1 layer and the underlying soil. Correlation is extended to the candidate layer in the Watong outcrop, which lies between deposits from the 15th–16th centuries and the 17th–19th centuries.

The dating results are refined by the modeled ages from the calculation results obtained using OxCal 4.4 (Fig. 7, Table 5; Ramsey, 2021). The modeled ages of the Shetoushan layers are 1444–1573 and 1524–1706, that form a continuous time span with the 1575 midpoint. A modeled interval of 12–227 years lies between the layers.

Collectively, the Chungtun-1 layer including the calculated boulder is attributed to the event that led to marine inundation and deposition in the 17th century (1575–1706, 1640±66). This event is reported for the first time in the study area and also in the South China Sea region. The candidate layer in Chungtun-2 outcrop records an earlier event that probably occurred in the late 15th–late 16th centuries (1444–1575, 1510±65). The source event was previously reported by Lu et al. (2019) based on the earlier finding of the upper Suogang layer. The coeval deposits in the Shetoushan and Chungtun-2 outcrops that were firstly examined in this study appear to constrain the northern extent of this marine inundation and deposition on the Penghu Islands (Fig. 1b).

已删除: of…wide range of densitiesy…and sizes range… includingfound in the…vesicular pumice, to ... [30]

已删除: of…the candidate gravel layers originated fromare…coastal marine environmentsin origin…and were reworked from the…beach–dune environments to the …igh supratidal location. The beach-derived sediments include mixed …ioclasts, such as comprising …oral, foraminifera, and mollusk, as well aswith…pumice, all of which are commonly observed on local beaches (Figs. 3a and 4a–c). On the Penghu Islands, M…odern beach pumice includes stranded rafts from the 2021 submarine eruption in the southern Izu-Bonin Arc, whereas pumice is absent in the Miocene basalt and sedimentary basement (Yen and Lee, 2017. (in Chinese with English abstract); Yu et al., 2022). Ancient stranded strands of …umice rafts are commonly incorporated into backshore event redepositions and have beenare…reported in northern Taiwan from the past 2.4 ka in northern Taiwan…(Yu et al., 2022). The redeposited dune and supratidal material is represented by angular basalt, brownish soil, and bioclastic sand in the matrix and is present in the sections below the candidateME ... [31]

已删除: TS…outcropsection…because of the continuous exposure, the…with two candidateME…layergravel occurrence…, ... [32]

已删除: …he lL…werayer…ME…hetoushanTS…layer-b…is intercalated into sandy soil dating from the 15th–early 17th centuries,,…with the ambient soil layers of the MESTS-a dating from the 16th–17th centuries and the 17th–19th centuries. …aterally, the MESTS-b …ayer is comparable in age to the candidate MECT-2 …ayer in(CT-2…outcrop)…Chungtun-2 which was deposited in 14th–15th centuries at the earliest based on the age of the detrital sediment matrix. The upper SuogangMESTS-b…layer is also in a comparable in…age to MESG-a (SG outcrop)… which …verlyingies…soil from the 13th–14th centuries. ... [33]

已删除: MESTS-a…is correlated with the ME…hungtunT…1 layer and the calculated boulderCTB (CT-1 outcrop)… which were deposited in the 16th–17th centuries, according to the dating results obtained for the ME…hungtunT…1 layer and the underlying soil. Correlation is extended toMESTS-a is also correlated…with …he candidate layer inMEWT…the (…aT…ong outcrop) ... [34]

已删除: ME…hetoushanTS-a…layernd b age… of …re 1444–1573 and 1524–1706, respectively, ... [35]

已删除: CTB and the ME…hungtunT…1 layerdeposits…including the calculated boulder isare…attributedprobably…tofrom…the event that led to marine inundation and deposition in the 17th century (1575–1706, 1640±66). This event is reported for the first time on Penghu Islands…n the study area and also in the South China Sea region. The MECT-2…andidate layer in the …T…ungtun-2 outcrop records an earlier event that probably occurred in the late 15th–late 16th centuries (1444–1575, 1510±65). The source eventCT-2 deposit…was reported upon …reviously reported by Lu et al. (2019), namely…based onas…thelayer…earlier finding of the upper ME…uogangG-a…layerin the SG outcrop (Lu et al., 2019)… The coeval deposits in the ShetoushanTS…and ChungtunT…2 outcrops that were firstly examined in this study appear to constrain the northern extent of this marine inundation and deposition onto ... [36]

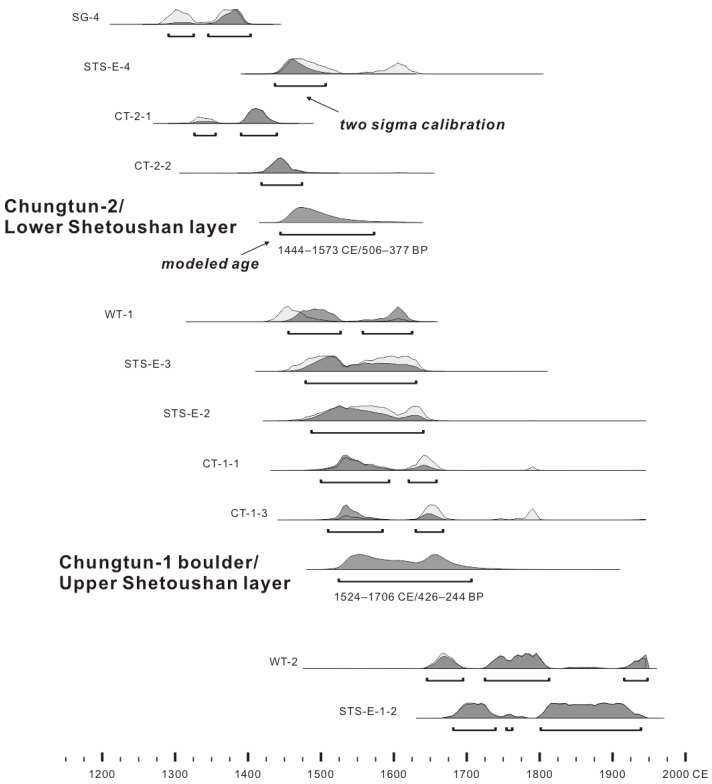

Figure 7: Modeled ages of the radiocarbon samples and the Chungtun-1 boulder/upper Shetoushan and Chungtun-2/lower Shetoushan layers obtained using OxCal v 4.4 (Ramsey, 2021). Further details are given in Table 5.

已删除: CTB

已删除: ME

已删除: TS-a

已删除: T

已删除: ME

已删除: TS-b

已删除: Calculation results of

已删除: from

已删除: as compared to the marine event layers and radiocarbon samples in this study

Table 5. Modeled ages of the radiocarbon samples and candidate event layers obtained using OxCal v. 4.4 program of Ramsey (2021).

Gravel layer and	Unmodeled ages (AD)			Modeled ages (AD)		
sample	from	to	%	from	to	%
SG	1281	1395	95.4	1291	1403	95.4
STS-E-4	1442	1631	95.4	1437	1506	95.4
CT-2-1	1322	1437	95.4	1326	1439	95.4
CT-2-2	1413	1480	95.4	1418	1474	95.4

Chungtun-2				1444	1573	95.4
WT-1	1426	1620	95.4	1455	1625	95.4
STS-E-3	1461	1636	95.4	1479	1630	95.4
STS-E-2	1484	1644	95.4	1487	1640	95.4
CT-1-1	1505	1795	95.4	1500	1658	95.4
Chungtun-1				1524	1706	95.4
WT-2	1643	…	95.4	1645	1948	95.4
STS-E-1-2	1682	1938	95.4	1681	1939	95.4

Interval	from	to	%
Chungtun-2-1	227	12	95.4

5 Discussion

5.1 Tsunami wave processes on the candidate gravel and boulder deposits

Integrating the results of the incorporative hydrodynamic approach and the facies-stratigraphic analysis indicates that the event depositions of both the Chungtun-1 and 2 gravel layers are attributed to tsunamis rather than typhoons.

Based on the size, shape, facies, elevation, and dating of Chungtun-1 boulder, the wave process is thought to have lifted the boulder from the intertidal joint-bounded exposure, transport it via incipient saltation and terminal rolling over a total distance of over 30 m, and significantly overflowed the cliff (Fig. 2). As a result, an estimated minimum wave height of 3.19 (~3.2) m is required. After calibrating the ancient local sea level and 100-year surge, the tallest typhoon waves (height = 0.73 × water depth) that can form in the Chungtun Channel are ruled out as insufficient for the boulder deposition. Typhoon waves reach only a maximum height of 3.3 m in the channel, which would only cause Chungtun-1 boulder to undergo slide–roll movement in the intertidal–subtidal zone (Table 3). The tallest typhoon waves in the supratidal zone may be less than 1.5 m high and too weak to push or roll the boulder onto the 2.5 m high cliff. Moreover, the typhoon waves that are likely to form in the channel are probably overestimated because the modeled ratio of 0.73 for wave height to water depth at wave break appears to be excessive (Collins, 1970). This is because the ratio tends to be small, at around 0.44–0.6, in nearly horizontal bathymetry such as that observed in the Penghu area (Fig. 1b; Noormets et al., 2004). This finding is supported by the wave height maximum that was set by the 2015 Super typhoon Soudelor, which decreased from 6.8 m in the 26-m-deep Paisha offshore to 6.5 m in the 14-m-deep Makong Channel and 2.8 m in the 8-m-deep Longman nearshore (Fig. 1b; Liu et al., 2016.(in Chinese with English abstract)). The ratio of 0.26–0.46 from these observations is probably more applicable to the Chungtun Channel. Accordingly, the tallest typhoon waves may have reached only 0.9–1.8 m in the channel during the 16th–17th centuries, which is barely enough to initiate Chungtun-1 boulder sliding in the intertidal–subtidal zone (Fig. 2c, Table 3).

已删除: MESTS-b
已删除: MESTS-a
已删除: MESTS
已删除: b
已删除: a
已删除: **CTB and**
已删除: with
已删除: T
已删除: B
已删除: the earlier CT-
已删除: event
已删除: the
已删除: CTB
已删除: CTB
已删除: ed
已删除: 0
已删除: (tsunami) or 12.0 m (typhoon)
已删除: stimat
已删除: using the Froude Numbers 2.0 and 1.0, respectively
已删除: high
已删除: 100
已删除: CT Channel
已删除: CTB
已删除: region
已删除: the
已删除: CTB
已删除: of
已删除: are
已删除: CTB
已删除: ,
已删除: as
已删除: offshore
已删除: at the
已删除: in
已删除: waterways
已删除: CT Channel
已删除: CT
已删除: C
已删除: CTB

The estimated wave period also associates the Chungtun-1 boulder transport with long-periodicity tsunami or tsunami-like composite waves (Table 3). The tsunami wave origin appears to be dominant over the tsunami-like composite wave, according to the facies characteristics of poor sorting, abundant fine-grained sediment, and matrix support (Figs. 3 and 6). The composite waves and induced currents usually have a low sediment capacity due to rapid attenuation following the wave break and low velocity as compared to tsunami waves (Watanabe et al., 2017; Dietrich et al., 2011; Bricker et al., 2014). Composite wave breaks tend to result in multiple overwashes and sublayers that are characterized by normal sedimentary grading and moderate-to-high sorting (Baumann et al., 2017; Brill et al., 2016; Sohn and Sohn, 2019). These features of better sorting and stratification are absent in the candidate gravel layers found in this study.

The supratidal elevation of most of the candidate gravel layers, 2.5–5.1 m a.s.l., also marks tsunami wave heights exceeding the 100-year typhoon surge of 1.8 m a.s.l. (Fig. 5a–b). The candidate layer elevation in the Watong and lower Shetoushan sections is only 2.0–2.1 m a.s.l., indicating the two layers may have been deposited by the 100-year surges in the 15th–17th centuries when the local sea level was 0.2–0.3 m higher (Chen and Liu, 1996). However, the modern surge maximum at 1.8 m a.s.l. that is associated with ongoing global warming may be too large to represent the surge conditions during the 17th–19th centuries of the Little Ice Age. It is because the historical surges at only 1.2–1.5 m a.s.l. are theoretically concordant with the cool climate control (Hsu, 2007. (in Chinese); Oey and Chou, 2016; Mei and Xie, 2016). Moreover, the Watong and lower Shetoushan layers are characterized by well-preserved articulated bivalves and gastropods, and feature depositions from rapid catastrophic events rather than prolonged storm depositions with intense collision and abrasion between shells and rock clasts (Fig. 6b and d; Donato et al., 2008; Madeira et al., 2020; Pérez-Torrado et al., 2006).

The estimated minimum tsunami waves that reach 3.2 m in height significantly surpass the modern record of 0.4 m height for the 1994 tsunami on the Penghu Islands. The wave height of several meters that is inferred from the paleotsunami deposits is not uncommon and has been recently reported both in the study area and in northern Taiwan (Yu et al., 2016; Lu et al., 2019; Sugawara et al., 2019). Despite the outcrops other than Chungtun-1 outcrop are barren of the cliff-top boulder, the elevation of candidate layers quantitatively marks the minimum tsunami wave run-up (Pignatelli et al., 2009; Nanayama and Shigeno, 2006; Paris et al., 2018). It is noteworthy that the present layer elevation was likely 0.2–0.3 m lower during deposition in the 15th–17th centuries when the local sea level was higher, and the beach profiles may shift landwards and upwards accordingly (Chen and Liu, 1996). Thus, the local wave height at Shetoushan outcrop during the 17th-century Chungtun-1 event is estimated at 2.4 m (Fig. 5a). The local wave height during the 16th-century Chungtun-2 event was probably 2.2 m at Chungtun-2 outcrop and 4.8 m at Suogang (Fig. 5a–b).

5.2 Probable event sources

Because no historical earthquake and tsunami are recorded on Penghu Islands, it probably indicates far-field sources for the Chungtun-1 and 2 events, such as the epicenter of the 1994 earthquake tsunami that is far away in the southwest Taiwan Strait (Fig. 1a). Across the Taiwan Strait, three distant candidate earthquakes with seawater overflows occurred in the period

已删除: CTB …hungtun-1 boulder transport with long-periodicity tsunami or tsunami-like composite waves (Table 3). The tsunami wave origin appears to be dominant over the tsunami-like composite wave, according to the facies characteristics of poor sorting, abundantrich suspension of…fine-grained sediment, and matrix (Figs. 3 and 6). The composite waves and induced currents usually have a low sediment capacity due to rapid attenuation following the wave break and low velocity as compared to tsunami waves (Watanabe et al., 2017; Dietrich et al., 2011; Bricker et al., 2014). Composite wave breaks tend to result in multiple overwashes and sublayers that are characterized by normal sedimentary grading and moderate-to-high sorting (Baumann et al., 2017; Brill et al., 2016; Sohn and Sohn, 2019). These features of better sorting and stratification are absent in the candidateME ... [37]

已删除: marine event…gravel layers, 2.5–5.1 m a.s.l., also marks tsunami inundation with…wave heights exceeding the 100 …00-year typhoon surge of 1.8 m a.s.l. (Fig. 5a–b). Among the layers…he candidate layer elevation in the , ME…atongT…and lower ME…hetoushanTS-b…sections isare…onlylower…at ….1 …– and ….10…m a.s.l., indicating the two layersrespectively, and…may have been deposited by the 100 ... [38]

已删除: under…the local sea level was 0.2–0.3 m highersea level high…(Chen and Liu, 1996). However, the modern surge maximum at 1.8 m a.s.l. that is associated with ongoing global warming may be too large to represent the surge conditions during the 17th–19th centuries of the Little Ice Age … It isin the 17th–19th centuries,…because the historical surges of …t only 1.2–1.5 m a.s.l. is …re theoretically concordant with the cool climate control (Hsu, 2007. (in Chinese); Oey and Chou, 2016; Mei and Xie, 2016). Moreover, the ME…atongT…and lower ME…hetoushanTS-l ... [40]

已設定格式 ... [39]

已删除: over ….0 … m in height significantly surpass the modern record of 0.4 m height for the 1994 tsunami, which reached high …onto …n the Penghu Islands. The wave height of several meters that is inferred from the paleotsunami deposits is not uncommon and has been recently reported both in the study area and in northern Taiwan (Yu et al., 2016; Lu et al., 2019; Sugawara et al., 2019). Despite the outcrops other than Chungtun-1 outcrop are barrenabsence…of the cliff-top boulders in the other outcrops… the supratidal …levation of candidatemarine gravel…layers marks the minimum tsunami wave run-up (Pignatelli et al., 2009; Nanayama and Shigeno, 2006; Paris et al., 2018). It is noteworthy that the present layer elevation was likely 0.2–0.3 m lower during deposition in the 15th–17th centuries when the local sea level was higher,…and the beach profiles may shift landwards and upwards accordingly (Chen and Liu, 1996). Thus, the local wave height in …tthe…ShetoushanTS…outcrop during the 17th-century ChungtunT…1B…event is estimated at 2.4 m (Fig. 5a). The local wave height during the 16th-century ChungtunT…2 event was probably 2.2 m at the …hungtunT…2 outcrop…outcrop and 4.8 m at the …uogangG outcrop ... [41]

已删除: CTB…and CT-… events, such as the epicenter of the 1994 earthquake tsunami that is far away in theat was distant…southwest Taiwan Straitoffshore to the SE ... [42]

of the two Chungtun events, namely the 1604 and 1640 earthquakes in southeast China and the 1661 earthquake in SW Taiwan (Keimatsu, 1963. (in Japanese with English abstract); Nakamura, 1935. (in Japanese); Lei and Ou, 1991. (in Chinese with English abstract)).

The newly identified 17th-century Chungtun-1 tsunami is tentatively associated with the 1661 earthquake based on the historical accounts and the results of comparison with the previously reported forward simulations. According to the estimated local wave height of 2.4–4.0 m, the Chungtun-1 tsunami was evidently much larger than the 0.4 m high tsunami ensuing the 1994 M6.4 earthquake (Central Weather Bureau, 2022). The 1640 earthquake and overflow are readily ruled out because they were insignificant and less disastrous than the 1604 and 1661 events (Keimatsu, 1963. (in Japanese with English abstract); Lei and Ou, 1991. (in Chinese with English abstract); Nakamura, 1935. (in Japanese)). The 1604 earthquake was previously associated with a shore-parallel northeast–southwest offshore rupture and an inferred magnitude of 8.0 near the southeast China coast (Fig. 1A; Lei and Ou, 1991. (in Chinese with English abstract)). However, the previously reported simulations of the earthquake mismatch the results of this study, showing a marked cross-strait wave dissipation from 0.96 m high in southeast China to 0.3 m high in northwest Taiwan (Huang et al., 2006. (in Chinese with English abstract); Wu, 2015. (in Chinese with English abstract)). The 1661 earthquake was the largest on southwest Taiwan and could be associated with the pronounced compressional tectonics of the orogenic island (Hsu, 2007. (in Chinese); Nakamura, 1935. (in Japanese)). The previously reported simulations feature 2–4 m high tsunamis in southwest Taiwan in association with scenarios of M8.2 earthquakes and reverse faulting and nonuniform slip distributions in the northern Manila Trench (Fig. 1a; Li et al., 2015). The estimated wave heights across southwest Taiwan and the Penghu Islands shown in the previous and the present studies are comparable and thus ought to be included in future studies.

The 16th-century Chungtun-2 tsunami has been previously correlated to the 1604 earthquake (Lu et al., 2019). However, based on the new dating results (1444–1575, 1510±65), it is now associated with an unidentified event, showing a significant age discrepancy. The 2.2–4.8 m wave height derived from the candidate layer elevation is reported for the first time and is comparable to the Chungtun-1 tsunami wave height, which likewise suggests a major event and calls for further investigation. One plausible explanation for the source of the tsunami is a submarine landslide, because steep slopes of high landslide potential are omnipresent from the Penghu Islands to SW Taiwan and no major historical earthquakes are recorded across the Taiwan Strait in the period under question (Fig. 1a). Future simulation that includes the Penghu Islands is important, as the previously reported landslide scenarios show 5-m-high tsunamis in SW Taiwan (Li et al., 2015; Liu et al., 2022).

6 Conclusions

The coastal tsunami impact of the South China Sea was quantitatively evaluated for the first time by applying the incipient motion formulas to the newly identified 17th century cliff-top boulder on Penghu Islands in the Taiwan Strait. This study distinguishes the tallest typhoon waves that can form in the interisland bathymetry during the co-occurrence of ancient high sea levels and a 100-year surge, and determines them to be too weak to account for the 2.5 m high cliff-top deposition. The

已删除: CT…events, namely the 1604 and 1640 earthquakes in southeastSE ... [43]

已删除: CTB …hungtun-1 tsunami is tentatively associated with the 1661 earthquake based on the historical accounts and the results of comparison with the previously reported forward simulations. According to the estimated local wave height of 2.4–4.0 m, the CTB …hungtun-1 tsunami was evidently much larger than the 0.4 m high tsunami ensuingthat was associated with…the 1994 M6.4 earthquake (Central Weather Bureau, 2022). The 1640 earthquake and overflow are readily ruled out because they were insignificant and less04 and 1661 earthquakes and overflows were probably more drastic and…disastrous than the 1604 and 166140…events 1963. (in Japanese with English abstract); Lei and Ou, 1991. (in Chinese with English abstract); Nakamura, 1935. (in Japanese)). The 1604 earthquake was previously associated with a shore-parallel northeastNE…southwestSW…offshore rupture and an inferredearthquake measuring…magnitude ofM…8.0 near the southeastSE…China coast (Fig. 1A; Lei and Ou, 1991. (in Chinese with English abstract)). However, tT…e previously reported simulations of the earthquake mismatch the results of this study, showing a marked cross-strait wave dissipation that varies…from 0.96 m in height…igh in southeastSE…China to 0.3 m high in northwestNW…Taiwan (Huang et al., 2006. (in Chinese with English abstract); Wu, 2015. (in Chinese with English abstract)). The 1661 earthquake was the largest on southwestthe …Taiwan orogen…andthat…couldan…be associated with the pronounced compressional tectonics of the orogenic islandin the 17th century…(Hsu, 2007. (in Chinese); Nakamura, 1935. (in Japanese)). The previously reported simulations feature 2–4 m high tsunamis in southwestSW…Taiwan in association with scenarios of M8.2 earthquakes and reverse faulting and nonuniform slip distributions in the northern Manila Trench (Fig. 1a; Li et al., 2015). The estimated wave heights across southwestSW ... [44]

已删除: CT…hungtun-2 tsunami has beenwas…previously correlated to the 1604 earthquake (Lu et al., 2019).,…However,and…is here tied to an unknown event …ased on the new dating results (1444–1575, 1510±65), it is now associated with an unidentified event, that …howings…a significant age discrepancy. The 2.2–4.8 m wave height derived from the candidate layer elevation is reported for the first time andt…2.2–4.8 m …s comparable to the Chungtun-1CTB…tsunami wave height, whichand…likewise suggests a majorsevere…event and that …alls for further investigationmore studies… One plausible explanation forSubmarine landslide may be one of…the top candidate…ource of the tsunami is a submarine landslide, because potentially ... [45]

已删除: ,…17th century,…cliff-top boulder on Penghu Islands in the Taiwan Strait. This studye…distinguishes the tallest tt…phoon waves that can form in the interisland bathymetry duringat…the co-occurrence of ancient high sea level high… and a 100 …00-year surge, and determines them to beare distinguished and found…too weak to account forresult in ... [46]

required tsunami height and period are estimated to be 3.2 m and 5.8 h, respectively, rendering boulder deposition and terminal rolling possible. Additionally, local gravel layers at three different locations indicate an inferred run-up wave height of 2.4–4.0 meters.

Compared to the other cliff-top boulders around the world (see Cox et al., 2020; Etienne et al., 2011; Goto et al., 2010 and references therein), the studied boulder is unique, and is characterized by a matrix-supported fabric, the upslope pinch-out bedform, and the lateral fining to pebble–cobble composition (Fig. 2). In addition to the angular boulder shape, the boulder facies record a suspension-rich turbulent flow process and the tsunami transport of bore-like waves from initial joint-bounded lift to saltation and rolling.

The newly obtained geological record obtained in this study improves our understanding of the South China Sea tsunamis and may contribute to future hydrodynamic simulations. The newly identified event during the period of 1575–1706 is related to the disastrous 1661 earthquake in southwest Taiwan, likely originating from megathrust activity in the northern Manila Trench (Fig. 1a). The previously reported event in the 15th–16th centuries is revised to have occurred between 1444–1575 and is correlated with an unspecified event, of which submarine landslide may be a prominent candidate because of the widespread steep slopes in the region (Lu et al., 2019).

已删除: at
已删除: 0
已删除: 6
已删除: is further inferred from the coeval gravel layers at three localities
已删除: the
已删除: Together with
已删除: s
已删除: in
已删除: period
已删除: SW
已删除: and probably
已删除: ed
已删除: by the modeled age of
已删除: to

Data availability:

The data are available upon request from the authors.

Author contribution:

NTY led the field investigation, calculated the hydrodynamic estimation, and drafted the manuscript. CHL and ICY participated the field survey and CHL carried out the DEM image of Chungtun Channel and boulder measurement. JHC undertook the grain size analysis. JYY and SJC provided important advises to the discussion and conclusions.

已删除: CT Channel

Competing interests:

The contact author has declared that none of the authors has any competing interests.

References

Barbano, M. S., Pirrotta, C., and Gerardi, F.: Large boulders along the south-eastern Ionian coast of Sicily: storm or tsunami deposits?, Mar. Geol., 275, 140–154, https://doi.org/10.1016/j.margeo.2010.05.005, 2010.
Baumann, J., Chaumillon, E., Bertin, X., Schneider, J.-L., Guillot, B., and Schmutz, M.: Importance of infragravity waves for the generation of washover deposits, Mar. Geol., 391, 20–35, https://doi.org/10.1016/j.margeo.2017.07.013, 2017.

Bricker, J. D., Takagi, H., Mas, E., Kure, S., Adriano, B., Yi, C., and Roeber, V.: Spatial variation of damage due to storm surge and waves during Typhoon Haiyan in the Philippines, J. Jpn. Soc. Civ. Eng., Ser. B2 (Coastal Engineering), 70, I_231–I_235, https://doi.org/10.2208/kaigan.70.I_231, 2014.

Brill, D., May, S. M., Engel, M., Reyes, M., Pint, A., Opitz, S., Dierick, M., Gonzalo, L. A., Esser, S., and Brückner, H.: Typhoon Haiyan's sedimentary record in coastal environments of the Philippines and its palaeotempestological implications, Nat. Hazards Earth Syst. Sci., 16, 2799–2822, https://doi.org/10.5194/nhess-16-2799-2016, 2016.

Central Weather Bureau: Wave Statistics, https://www.cwb.gov.tw/V8/E/C/MMC_STAT/sta_wave.html, 2022.

Chang, H. M.: On the reoccurrence period of joint events of typhoon waves and surges, Department of Hydraulic and Ocean Engineering, National Cheng Kung University, 110 pp., 2009. (in Chinese with English abstract).

Chen, Y.-G. and Liu, T.-K.: Sea level changes in the last several thousand years, Penghu Islands, Taiwan Strait, Quat. Res., 45, 254–262, https://doi.org/10.1006/qres.1996.0026, 1996.

Collins, J. I.: Probabilities of breaking wave characteristics, in: Coastal Engineering 1970, 1970 American Society of Civil Engineers, 399–414, https://doi.org/10.1061/9780872620285.025, 1970.

Cox, R., Ardhuin, F., Dias, F., Autret, R., Beisiegel, N., Earlie, C. S., Herterich, J. G., Kennedy, A., Paris, R., Raby, A., Schmitt, P., and Weiss, R.: Systematic review shows that work done by storm waves can be misinterpreted as tsunami-related because commonly used hydrodynamic equations are flawed, Front. Mar. Sci., 7, https://doi.org/10.3389/fmars.2020.00004, 2020.

Dietrich, J. C., Zijlema, M., Westerink, J. J., Holthuijsen, L. H., Dawson, C., Luettich, R. A., Jensen, R. E., Smith, J. M., Stelling, G. S., and Stone, G. W.: Modeling hurricane waves and storm surge using integrally-coupled, scalable computations, Coast. Eng., 58, 45–65, https://doi.org/10.1016/j.coastaleng.2010, 2011.

Donato, S. V., Reinhardt, E. G., Boyce, J. I., Rothaus, R., and Vosmer, T.: Identifying tsunami deposits using bivalve shell taphonomy, Geology, 36, 199–202, https://doi.org/10.1130/g24554a.1, 2008.

Etienne, S., Buckley, M., Paris, R., Nandasena, A. K., Clark, K., Strotz, L., Chagué-Goff, C., Goff, J., and Richmond, B.: The use of boulders for characterising past tsunamis: Lessons from the 2004 Indian Ocean and 2009 South Pacific tsunamis, Earth Sci. Rev., 107, 76–90, https://doi.org/10.1016/j.earscirev.2010.12.006, 2011.

Fujiwara, O. and Kamataki, T.: Chapter nine - Tsunami depositional processes reflecting the waveform in a Small Bay: Interpretation from the grain-size distribution and sedimentary structures, in: Tsunamiites, edited by: Shiki, T., Tsuji, Y., Yamazaki, T., and Minoura, K., Elsevier, Amsterdam, 133–152, http://dx.doi.org/10.1016/B978-0-444-51552-0.00009-6, 2008.

Goff, J., Witter, R., Terry, J., and Spiske, M.: Palaeotsunamis in the Sino-Pacific region, Earth Sci. Rev., 210, 103352, https://doi.org/10.1016/j.earscirev.2020.103352, 2020.

Goto, K., Kawana, T., and Imamura, F.: Historical and geological evidence of boulders deposited by tsunamis, southern Ryukyu Islands, Japan, Earth Sci. Rev., 102, 77–99, https://doi.org/10.1016/j.earscirev.2010.06.005, 2010.

Goto, K., Okada, K., and Imamura, F.: Characteristics and hydrodynamics of boulders transported by storm waves at Kudaka Island, Japan, Mar. Geol., 262, 14–24, https://doi.org/10.1016/j.margeo.2009.03.001, 2009.

Hsu, H., Chen, C. F. (Ed.): Renewed editions of Qiing dynastic historical accounts of Taiwan natural hazards, Taiwan Strait Reserach Series, Fujian People's publishing house, Fuchou, PROC, , 396 pp.2007. (in Chinese).

Huang, Z., Wang, S. X., and Wang, X. N.: Analysis of the 1604 Quanzhou offshore earthquake-tsunami effects, Earthquake, 26, 94–102, 2006. (in Chinese with English abstract).

Hudson, R. Y.: Wave forces on breakwaters, Trans. Am. Soc. Civil Eng., 118, 653–674, https://doi.org/10.1061/TACEAT.0006816, 1953.

Imamura, F., Goto, K., and Ohkubo, S.: A numerical model for the transport of a boulder by tsunami, J. Geophys. Res. Oceans, 113, https://doi.org/10.1029/2007JC004170, 2008.

Jiang, W. D., Chang, H. K., Liou, J. C., Chen, W. W., and Ho, L. S.: Investigation of long-term wave statistics and design wave for main harbors of Taiwan. Report of institute of transportation, MOTC, Taiwan, 2/4, No. 100–52–7537, Taipei, 246, 2011. (in Chinese with English abstract).

Jiang, W. D., Chang, H. K., Liou, J. C., Chen, W. W., and Ho, L. S.: Investigation of long-term wave statistics and design wave for main harbors of Taiwan. Report of institute of transportation, MOTC, Taiwan, 3/4, No. 101–16–7590, Taipei, 246, 2012. (in Chinese with English abstract).

Keimatsu, M.: On the historical tidal waves in China, Zisin, J. Seismol. Soc. Jpn. 2nd ser., 16, 149–160, 1963. (in Japanese with English abstract).
Kennedy, A. B., Cox, R., and Dias, F.: Storm waves may be the source of some "tsunami" coastal boulder deposits, Geophys. Res. Lett., 48, e2020GL090775, https://doi.org/10.1029/2020GL090775, 2021.
Lau, A. Y. A., Switzer, A. D., Dominey-Howes, D., Aitchison, J. C., and Zong, Y.: Written records of historical tsunamis in the northeastern South China Sea - challenges associated with developing a new integrated database, Nat. Hazards Earth Syst. Sci., 10, 1793–1806, https://doi.org/10.5194/nhess-10-1793-2010, 2010.
Lei, T. C. and Ou, B. S.: Earthquake and sea overflow in Taiwan Strait and its adjacent regions, J. Oceanogr. Taiwan Strait, 10, 264–270, 1991. (in Chinese with English abstract).
Li, L. L., Shi, F. Y., Ma, G. F., and Qiu, Q.: Tsunamigenic potential of the Baiyun slide complex in the South China Sea, J. Geophys. Res., 124, 7680–7698, https://doi.org/10.1029/2019JB018062, 2019.
Li, L. L., Switzer, A. D., Chan, C. H., Wang, Y., Weiss, R., and Qiu, Q.: How heterogeneous coseismic slip affects regional probabilistic tsunami hazard assessment: A case study in the South China Sea, J. Geophys. Res., 121, 6250–6272, https://doi.org/10.1002/2016JB013111, 2016.
Li, L. L., Switzer, A. D., Wang, Y., Weiss, R., Qiu, Q., Chan, C. H., and Tapponnier, P.: What caused the mysterious eighteenth century tsunami that struck the southwest Taiwan coast?, Geophys. Res. Lett., 42, 8498–8506, https://doi.org/10.1002/2015GL065567, 2015.
Liu, C. C., Lee, J. F., Lee, C. Y., Chen, M. T., and Su, C. H.: Development of an operational wind wave simulation system for Penghu sea areas, The 38th Ocean Engineering Conference in Taiwan, Taipei, Taiwan, 101–106, 2016.
Liu, T. C., Wu, T. R., and Hsu, S. K.: Historical tsunamis of Taiwan in the 18th century: the 1781 Jiateng Harbor flooding and 1782 tsunami event, Nat. Hazards Earth Syst. Sci., 22, 2517–2530, https://doi.org/10.5194/nhess-22-2517-2022, 2022.
Lorang, M. S.: A wave-competence approach to distinguish between boulder and megaclast deposits due to storm waves versus tsunamis, Mar. Geol., 283, 90–97, http://dx.doi.org/10.1016/j.margeo.2010.10.005, 2011.
Lowe, D. R.: Sediment gravity flows; II, Depositional models with special reference to the deposits of high-density turbidity currents, J. Sed. Res., 52, 279–297, https://doi.org/10.1306/212F7F31-2B24-11D7-8648000102C1865D, 1982.
Lu, C.-H., Yen, J.-Y., Chyi, S.-J., Yu, N.-T., and Chen, J.-H.: Geological records of South China Sea tsunamis on Penghu Islands, Taiwan, J. Asian Earth Sci., 177, 263–274, https://doi.org/10.1016/j.jseaes.2019.02.027, 2019.
Madeira, J., Ramalho, R. S., Hoffmann, D. L., Mata, J., and Moreira, M.: A geological record of multiple Pleistocene tsunami inundations in an oceanic island: The case of Maio, Cape Verde, Sedimentology, 67, 1529-1552, https://doi.org/10.1111/sed.12612, 2020.
Megawati, K., Shaw, F., Sieh, K., Huang, Z., Wu, T.-R., Lin, Y., Tan, S. K., and Pan, T.-C.: Tsunami hazard from the subduction megathrust of the South China Sea: Part I. Source characterization and the resulting tsunami, J. Asian Earth Sci., 36, 13-20, https://doi.org/10.1016/j.jseaes.2008.11.012, 2009.
Mei, W. and Xie, S. P.: Intensification of landfalling typhoons over the northwest Pacific since the late 1970s, Nat. Geosci., 9, 753–757, https://doi.org/10.1038/ngeo2792, 2016.
Nakamura, M., Arashiro, Y., and Shiga, S.: Numerical simulations to account for boulder movements on Lanyu Island, Taiwan: tsunami or storm?, Earth, Planets Space, 66, 1–20, https://doi.org/10.1186/1880-5981-66-128, 2014.
Nakamura, T.: Taiwan earthquake accounts in Dutch documents, Kagaku no Taiwan, 6–10, 1935. (in Japanese).
Nanayama, F. and Shigeno, K.: Inflow and outflow facies from the 1993 tsunami in southwest Hokkaido, Sediment. Geol., 187, 139–158, https://doi.org/10.1016/j.sedgeo.2005.12.024, 2006.
Nandasena, N. A. K.: Chapter 29: Perspective of incipient motion formulas: boulder transport by high-energy waves, in: Geological records of tsunamis and other extreme waves, in: Geological records of tsunamis and other extreme waves, edited by: Engel, M., Pilarczyk, J., May, S. M., Brill, D., and Garrett, E., Elsevier, 641–659, https://doi.org/10.1016/B978-0-12-815686-5.00029-8, 2020.
Nandasena, N. A. K., Paris, R., and Tanaka, N.: Reassessment of hydrodynamic equations: Minimum flow velocity to initiate boulder transport by high energy events (storms, tsunamis), Mar. Geol., 281, 70–84, 10.1016/j.margeo.2011.02.005, 2011.
Nandasena, N. A. K., Scicchitano, G., Scardino, G., Milella, M., Piscitelli, A., and Mastronuzzi, G.: Boulder displacements along rocky coasts: A new deterministic and theoretical approach to improve incipient motion formulas, Geomorphology, 407, https://doi.org/10.1016/j.geomorph.2022.108217, 2022.

Noormets, R., Crook, K. A., and Felton, E. A.: Sedimentology of rocky shorelines: 3.: Hydrodynamics of megaclast emplacement and transport on a shore platform, Oahu, Hawaii, Sediment. Geol., 172, 41–65, https://doi.org/10.1016/j.sedgeo.2004.07.006, 2004.
Nott, J.: Waves, coastal boulder deposits and the importance of the pre-transport setting, Earth Planet. Sci. Lett., 210, 269–276, https://doi.org/10.1016/S0012-821X(03)00104-3, 2003.
Oey, L. Y. and Chou, S.: Evidence of rising and poleward shift of storm surge in western North Pacific in recent decades, J. Geophys. Res., 121, 5181–5192, https://doi.org/10.1002/2016JC011777, 2016.
Okal, E. A., Synolakis, C. E., and Kalligeris, N.: Tsunami simulations for regional sources in the South China and adjoining seas, Pure Appl. Geophys., 168, 1153–1173, https://doi.org/10.1007/s00024-010-0230-x, 2011.
Paris, R., Ramalho, R. S., Madeira, J., Ávila, S., May, S. M., Rixhon, G., Engel, M., Brückner, H., Herzog, M., Schukraft, G., Perez-Torrado, F. J., Rodriguez-Gonzalez, A., Carracedo, J. C., and Giachetti, T.: Mega-tsunami conglomerates and flank collapses of ocean island volcanoes, Mar. Geol., 395, 168–187, https://doi.org/10.1016/j.margeo.2017.10.004, 2018.
Pérez-Torrado, F. J., Paris, R., Cabrera, M. C., Schneider, J.-L., Wassmer, P., Carracedo, J.-C., Rodríguez-Santana, Á., and Santana, F.: Tsunami deposits related to flank collapse in oceanic volcanoes: The Agaete Valley evidence, Gran Canaria, Canary Islands, Mar. Geol., 227, 135-149, https://doi.org/10.1016/j.margeo.2005.11.008, 2006.
Pignatelli, C., Sansò, P., and Mastronuzzi, G.: Evaluation of tsunami flooding using geomorphologic evidence, Mar. Geol., 260, 6–18, https://doi.org/10.1016/j.margeo.2009.01.002, 2009.
Qiu, Q., Li, L. L., Hsu, Y. J., Wang, Y., Chan, C. H., and Switzer, A. D.: Revised earthquake sources along Manila Trench for tsunami hazard assessment in the South China Sea, Nat. Hazards Earth Syst. Sci., 19, 1565–1583, https://doi.org/10.5194/nhess-19-1565-2019, 2019.
Ramos, N. T., Maxwell, K. V., Tsutsumi, H., Chou, Y.-C., Duan, F., Shen, C.-C., and Satake, K.: Occurrence of 1 ka-old corals on an uplifted reef terrace in west Luzon, Philippines: Implications for a prehistoric extreme wave event in the South China Sea region, Geosci. Lett., 4, 1–13, https://doi.org/10.1186/s40562-017-0078-3, 2017.
Ramsey, C. B.: The OxCal program v 4.4, The Oxford Radiocarbon Acceleration Unit, University of Oxford [code], https://c14.arch.ox.ac.uk/oxcal/OxCal.html, 2021.
Reimer, P. J., Bard, E., Bayliss, A., Beck, J. W., Blackwell, P. G., Ramsey, C. B., Buck, C. E., Cheng, H., Edwards, R. L., Friedrich, M., Grootes, P. M., Guilderson, T. P., Haflidason, H., Hajdas, I., Hatté, C., Heaton, T. J., Hoffmann, D. L., Hogg, A. G., Hughen, K. A., Kaiser, K. F., Kromer, B., Manning, S. W., Niu, M., Reimer, R. W., Richards, D. A., Scott, E. M., Southon, J. R., Staff, R. A., Turney, C. S. M., and van der Plicht, J.: IntCal13 and Marine13 Radiocarbon Age Calibration Curves 0–50,000 Years Cal BP, Radiocarbon, 55, 1869–1887, https://doi.org/10.2458/azu_js_rc.55.16947, 2013.
Sohn, C. and Sohn, Y. K.: Volcaniclastic tide-modulated tempestite in a coastal tuff ring, Jeju Island, Korea, Sci. Rep., 9, 1–7, https://doi.org/10.1038/s41598-019-39784-0, 2019.
Sugawara, D., Yu, N. T., and Yen, J. Y.: Estimating a tsunami source by sediment transport modeling: A primary attempt on a historical/1867 Normal-Faulting Tsunami in Northern Taiwan, J. Geophys. Res., 124, 1675–1700, https://doi.org/10.1029/2018JF004831, 2019.
Sun, L. G., Zhou, X., Huang, W., Liu, X. D., Yan, H., Xie, Z. Q., Wu, Z. J., Zhao, S. P., Shao, D., and Yang, W. Q.: Preliminary evidence for a 1000-year-old tsunami in the South China Sea, Sci. Rep., 3, 1–5, https://doi.org/10.1038/srep01655, 2013.
Terry, J. P., Winspear, N., Goff, J., and Tan, P. H. H.: Past and potential tsunami sources in the South China Sea: A brief synthesis, Earth Sci. Rev., 167, 47–61, https://doi.org/10.1016/j.earscirev.2017.02.007, 2017.
Watanabe, M., Bricker, J. D., Goto, K., and Imamura, F.: Factors responsible for the limited inland extent of sand deposits on Leyte Island during 2013 Typhoon Haiyan, J. Geophys. Res., 122, 2795–2812, https://doi.org/10.1002/2016JC012023, 2017.
Wu, T. R.: Impact intensity analysis on the 1604 Quanzhou earthquake tsunami and the impacts to the western coast of Taiwan, National Central University, Taipei CityMOTC-CWB-104-E-19, 45, 2015. (in Chinese with English abstract).
Wu, T. R. and Huang, H. C.: Modeling tsunami hazards from Manila Trench to Taiwan, J. Asian Earth Sci., 36, 21–28, https://doi.org/10.1016/j.jseaes.2008.12.006, 2009.
Yang, W. Q., Sun, L., Yang, Z., Gao, S., Gao, Y., Shao, D., Mei, Y., Zang, J., Wang, Y., and Xie, Z.: Nan'ao, an archaeological site of Song dynasty destroyed by tsunami, Chin. Sci. Bull., 64, 107–120, https://doi.org/10.1360/N972018-00740, 2019.

Yen, I. C. and Lee, C. Y.: Geologic map and explanatory text of Taiwan scale 1:50,000, 73–76, Penghu Islands, Central Geological Survey, MOEA, R.O.C., 104 (in Chinese with English abstract) pp.2017. (in Chinese with English abstract).
Yen, I. C. and Lee, C. Y.: Geologic map and explanatory text of Taiwan scale 1:50,000, 73–76, Penghu Islands, Central Geological Survey, MOEA, R.O.C., 97 (in Chinese with English Abstract) pp.2018.
Yu, N.-T., Yen, J.-Y., Yen, I. C., and Chu, M.-F.: An extended, 2.4-ka long record of western Pacific tsunamis and pumice rafts in northern Taiwan: Tsunami recurrence, pumice sources, and drifting routes, Quat. Sci. Rev., 281, 107423, https://doi.org/10.1016/j.quascirev.2022.107423, 2022.
Yu, N. T., Yen, J. Y., Chen, W. S., Yen, I. C., and Liu, J. H.: Geological records of western Pacific tsunamis in northern Taiwan: AD 1867 and earlier event deposits, Mar. Geol., 372, 1–16, http://dx.doi.org/10.1016/j.margeo.2015.11.010, 2016.
Yu, S.-B., Chen, H.-Y., and Kuo, L.-C.: Velocity field of GPS stations in the Taiwan area, Tectonophysics, 274, 41–59, https://doi.org/10.1016/S0040-1951(96)00297-1, 1997.

第 1 頁: [1] 已刪除　　游能悌　　2023/6/10 12:15:00 PM

第 1 頁: [1] 已刪除　　游能悌　　2023/6/10 12:15:00 PM

第 1 頁: [1] 已刪除　　游能悌　　2023/6/10 12:15:00 PM

第 1 頁: [1] 已刪除　　游能悌　　2023/6/10 12:15:00 PM

第 1 頁: [1] 已刪除　　游能悌　　2023/6/10 12:15:00 PM

第 1 頁: [1] 已刪除　　游能悌　　2023/6/10 12:15:00 PM

第 1 頁: [1] 已刪除　　游能悌　　2023/6/10 12:15:00 PM

第 1 頁: [1] 已刪除　　游能悌　　2023/6/10 12:15:00 PM

第 1 頁: [1] 已刪除　　游能悌　　2023/6/10 12:15:00 PM

第 1 頁: [1] 已刪除　　游能悌　　2023/6/10 12:15:00 PM

第 1 頁: [1] 已刪除　　游能悌　　2023/6/10 12:15:00 PM

第 1 頁: [1] 已刪除　　游能悌　　2023/6/10 12:15:00 PM

第 1 頁: [1] 已刪除　　游能悌　　2023/6/10 12:15:00 PM

第 1 頁: [1] 已刪除　　游能悌　　2023/6/10 12:15:00 PM

第 1 頁: [1] 已刪除　　游能悌　　2023/6/10 12:15:00 PM

第 1 頁: [1] 已刪除　　游能悌　　2023/6/10 12:15:00 PM

第 1 頁: [1] 已刪除　　游能悌　　2023/6/10 12:15:00 PM

第 1 頁: [1] 已刪除　　游能悌　　2023/6/10 12:15:00 PM

第 1 頁: [1] 已刪除　　游能悌　　2023/6/10 12:15:00 PM

第 1 頁: [1] 已刪除　　游能悌　　2023/6/10 12:15:00 PM

第 1 頁: [1] 已刪除　　游能悌　　2023/6/10 12:15:00 PM

第 1 頁: [1] 已刪除　　游能悌　　2023/6/10 12:15:00 PM

第 1 頁: [1] 已刪除　　游能悌　　2023/6/10 12:15:00 PM

第 1 頁: [1] 已刪除　　游能悌　　2023/6/10 12:15:00 PM

第 1 頁: [1] 已刪除　　游能悌　　2023/6/10 12:15:00 PM

第 1 頁: [1] 已刪除　　游能悌　　2023/6/10 12:15:00 PM

第 1 頁: [1] 已刪除　　游能悌　　2023/6/10 12:15:00 PM

第 1 頁: [1] 已刪除　　游能悌　　2023/6/10 12:15:00 PM

第 1 頁: [1] 已刪除　　游能悌　　2023/6/10 12:15:00 PM

第 1 頁: [1] 已刪除　　游能悌　　2023/6/10 12:15:00 PM

第 1 頁: [1] 已刪除　　游能悌　　2023/6/10 12:15:00 PM

第 1 頁: [1] 已刪除　　游能悌　　2023/6/10 12:15:00 PM

第 1 頁: [1] 已刪除　　游能悌　　2023/6/10 12:15:00 PM

第 1 頁: [1] 已刪除　　游能悌　　2023/6/10 12:15:00 PM

第 1 頁: [1] 已刪除　　游能悌　　2023/6/10 12:15:00 PM

第 1 頁: [1] 已刪除　　游能悌　　2023/6/10 12:15:00 PM

第 1 頁: [2] 已刪除　　游能悌　　2023/6/10 12:30:00 PM

第 1 頁: [2] 已刪除　　游能悌　　2023/6/10 12:30:00 PM

第 1 頁: [2] 已刪除　　游能悌　　2023/6/10 12:30:00 PM

第 1 頁: [2] 已刪除　　游能悌　　2023/6/10 12:30:00 PM

第 1 頁: [2] 已刪除　　游能悌　　2023/6/10 12:30:00 PM

第 1 頁: [2] 已刪除　　游能悌　　2023/6/10 12:30:00 PM

第 2 頁: [3] 已刪除　　游能悌　　2023/6/10 12:32:00 PM

第 2 頁: [3] 已刪除　　游能悌　　2023/6/10 12:32:00 PM

第 2 頁: [3] 已刪除　　游能悌　　2023/6/10 12:32:00 PM

第 2 頁: [3] 已刪除　　游能悌　　2023/6/10 12:32:00 PM

第 2 頁: [4] 已刪除　　游能悌　　2023/6/10 12:33:00 PM

第 2 頁: [4] 已刪除　　游能悌　　2023/6/10 12:33:00 PM

第 2 頁: [4] 已刪除　　游能悌　　2023/6/10 12:33:00 PM

第 2 頁: [4] 已刪除　　游能悌　　2023/6/10 12:33:00 PM

第 2 頁: [4] 已刪除　　游能悌　　2023/6/10 12:33:00 PM

第 2 頁: [4] 已刪除　　游能悌　　2023/6/10 12:33:00 PM

第 2 頁: [4] 已刪除　　游能悌　　2023/6/10 12:33:00 PM

第 2 頁: [4] 已刪除　　游能悌　　2023/6/10 12:33:00 PM

第 2 頁: [4] 已刪除　　游能悌　　2023/6/10 12:33:00 PM

第 2 頁: [4] 已刪除　　游能悌　　2023/6/10 12:33:00 PM

第 2 頁: [4] 已刪除　　游能悌　　2023/6/10 12:33:00 PM

第 2 頁: [4] 已刪除　　游能悌　　2023/6/10 12:33:00 PM

第 2 頁: [4] 已刪除　　游能悌　　2023/6/10 12:33:00 PM

第 2 頁: [4] 已刪除　　游能悌　　2023/6/10 12:33:00 PM

第 2 頁: [4] 已刪除　　游能悌　　2023/6/10 12:33:00 PM

第 2 頁: [4] 已刪除　　游能悌　　2023/6/10 12:33:00 PM

第 2 頁: [4] 已刪除　　游能悌　　2023/6/10 12:33:00 PM

第 2 頁: [4] 已刪除　　游能悌　　2023/6/10 12:33:00 PM

第 2 頁: [5] 已刪除　　游能悌　　2023/6/10 12:39:00 PM

第 2 頁: [5] 已刪除　　游能悌　　2023/6/10 12:39:00 PM

第 2 頁: [5] 已刪除　　游能悌　　2023/6/10 12:39:00 PM

第 2 頁: [5] 已刪除　　游能悌　　2023/6/10 12:39:00 PM

第 2 頁: [5] 已刪除　　游能悌　　2023/6/10 12:39:00 PM

第 2 頁: [5] 已刪除　　游能悌　　2023/6/10 12:39:00 PM

第 2 頁: [5] 已刪除　　游能悌　　2023/6/10 12:39:00 PM

第 2 頁: [5] 已刪除　　游能悌　　2023/6/10 12:39:00 PM

第 2 頁: [5] 已刪除　　游能悌　　2023/6/10 12:39:00 PM

第 2 頁: [5] 已刪除　　游能悌　　2023/6/10 12:39:00 PM

第 2 頁: [5] 已刪除　　游能悌　　2023/6/10 12:39:00 PM

第 2 頁: [5] 已刪除　　游能悌　　2023/6/10 12:39:00 PM

第 2 頁: [5] 已刪除　　游能悌　　2023/6/10 12:39:00 PM

第 2 頁: [6] 已刪除　　游能悌　　2023/6/10 12:44:00 PM

第 2 頁: [6] 已刪除　　游能悌　　2023/6/10 12:44:00 PM

第 2 頁: [6] 已刪除　　游能悌　　2023/6/10 12:44:00 PM

第 2 頁: [6] 已刪除　　游能悌　　2023/6/10 12:44:00 PM

第 2 頁: [6] 已刪除　　游能悌　　2023/6/10 12:44:00 PM

第 2 頁: [6] 已刪除　　游能悌　　2023/6/10 12:44:00 PM

第 2 頁: [6] 已刪除　　游能悌　　2023/6/10 12:44:00 PM

第 2 頁: [6] 已刪除　　游能悌　　2023/6/10 12:44:00 PM

第 2 頁: [6] 已刪除　　游能悌　　2023/6/10 12:44:00 PM

第 2 頁: [6] 已刪除　　游能悌　　2023/6/10 12:44:00 PM

第 2 頁: [6] 已刪除　　游能悌　　2023/6/10 12:44:00 PM

第 2 頁: [6] 已刪除　　游能悌　　2023/6/10 12:44:00 PM

第 2 頁: [6] 已刪除　　游能悌　　2023/6/10 12:44:00 PM

第 2 頁: [6] 已刪除　　游能悌　　2023/6/10 12:44:00 PM

第 4 頁: [7] 已刪除　　游能悌　　2023/3/13 2:08:00 PM

第 4 頁: [7] 已刪除　　游能悌　　2023/3/13 2:08:00 PM

第 4 頁: [7] 已刪除　　游能悌　　2023/3/13 2:08:00 PM

第 4 頁: [7] 已刪除　　游能悌　　2023/3/13 2:08:00 PM

第 4 頁: [7] 已刪除　　游能悌　　2023/3/13 2:08:00 PM

第 4 頁: [7] 已刪除　　游能悌　　2023/3/13 2:08:00 PM

第 4 頁: [7] 已刪除　　游能悌　　2023/3/13 2:08:00 PM

第 4 頁: [7] 已刪除　　游能悌　　2023/3/13 2:08:00 PM

第 4 頁: [7] 已刪除　　游能悌　　2023/3/13 2:08:00 PM

第 4 頁: [7] 已刪除　　游能悌　　2023/3/13 2:08:00 PM

第 4 頁: [7] 已刪除　　游能悌　　2023/3/13 2:08:00 PM

第 4 頁: [7] 已刪除　　游能悌　　2023/3/13 2:08:00 PM

第 4 頁: [7] 已刪除　　游能悌　　2023/3/13 2:08:00 PM

第 4 頁: [7] 已刪除　　游能悌　　2023/3/13 2:08:00 PM

第 4 頁: [7] 已刪除　　游能悌　　2023/3/13 2:08:00 PM

第 4 頁: [7] 已刪除　　游能悌　　2023/3/13 2:08:00 PM

第 4 頁: [7] 已刪除　　游能悌　　2023/3/13 2:08:00 PM

第 4 頁: [7] 已刪除　　游能悌　　2023/3/13 2:08:00 PM

第 4 頁: [7] 已刪除　　游能悌　　2023/3/13 2:08:00 PM

第 4 頁: [7] 已刪除　　游能悌　　2023/3/13 2:08:00 PM

第 4 頁: [7] 已刪除　　游能悌　　2023/3/13 2:08:00 PM

第 4 頁: [7] 已刪除　　游能悌　　2023/3/13 2:08:00 PM

第 4 頁: [7] 已刪除　　游能悌　　2023/3/13 2:08:00 PM

第 4 頁: [7] 已刪除　　游能悌　　2023/3/13 2:08:00 PM

第 4 頁: [8] 已刪除　　游能悌　　2023/5/21 4:00:00 PM

第 4 頁: [8] 已刪除　　游能悌　　2023/5/21 4:00:00 PM

第 4 頁: [8] 已刪除　　游能悌　　2023/5/21 4:00:00 PM

第 4 頁: [8] 已刪除　　游能悌　　2023/5/21 4:00:00 PM

第 4 頁: [8] 已刪除　　游能悌　　2023/5/21 4:00:00 PM

第 4 頁: [8] 已刪除　　游能悌　　2023/5/21 4:00:00 PM

第 4 頁: [8] 已刪除　　游能悌　　2023/5/21 4:00:00 PM

第 4 頁: [8] 已刪除　　游能悌　　2023/5/21 4:00:00 PM

第 4 頁: [8] 已刪除　　游能悌　　2023/5/21 4:00:00 PM

第 4 頁: [8] 已刪除　　游能悌　　2023/5/21 4:00:00 PM

第 4 頁: [8] 已刪除　　游能悌　　2023/5/21 4:00:00 PM

第 4 頁: [8] 已刪除　　游能悌　　2023/5/21 4:00:00 PM

第 4 頁: [8] 已刪除　　游能悌　　2023/5/21 4:00:00 PM

第 4 頁: [9] 已刪除　　游能悌　　2023/6/4 8:34:00 PM

第 4 頁: [9] 已刪除　　游能悌　　2023/6/4 8:34:00 PM

第 4 頁: [9] 已刪除　　游能悌　　2023/6/4 8:34:00 PM

第 4 頁: [9] 已刪除　　游能悌　　2023/6/4 8:34:00 PM

第 4 頁: [9] 已刪除　　游能悌　　2023/6/4 8:34:00 PM

第 4 頁: [9] 已刪除　　游能悌　　2023/6/4 8:34:00 PM

第 4 頁: [9] 已刪除　　游能悌　　2023/6/4 8:34:00 PM

第 4 頁: [9] 已刪除　　游能悌　　2023/6/4 8:34:00 PM

第 4 頁: [9] 已刪除　　游能悌　　2023/6/4 8:34:00 PM

第 4 頁: [9] 已刪除　　游能悌　　2023/6/4 8:34:00 PM

第 4 頁: [9] 已刪除　　游能悌　　2023/6/4 8:34:00 PM

第 4 頁: [9] 已刪除　　游能悌　　2023/6/4 8:34:00 PM

第 4 頁: [9] 已刪除　　游能悌　　2023/6/4 8:34:00 PM

第 4 頁: [9] 已刪除　　游能悌　　2023/6/4 8:34:00 PM

第 4 頁: [9] 已刪除　　游能悌　　2023/6/4 8:34:00 PM

第 4 頁: [9] 已刪除　　游能悌　　2023/6/4 8:34:00 PM

第 4 頁: [9] 已刪除　　游能悌　　2023/6/4 8:34:00 PM

第 4 頁: [9] 已刪除　　游能悌　　2023/6/4 8:34:00 PM

第 4 頁: [10] 已刪除　游能悌　2023/6/4 8:37:00 PM

第 4 頁: [10] 已刪除　游能悌　2023/6/4 8:37:00 PM

第 4 頁: [10] 已刪除　游能悌　2023/6/4 8:37:00 PM

第 4 頁: [10] 已刪除　游能悌　2023/6/4 8:37:00 PM

第 4 頁: [10] 已刪除　游能悌　2023/6/4 8:37:00 PM

第 4 頁: [10] 已刪除　游能悌　2023/6/4 8:37:00 PM

第 4 頁: [10] 已刪除　游能悌　2023/6/4 8:37:00 PM

第 4 頁: [10] 已刪除　游能悌　2023/6/4 8:37:00 PM

第 4 頁: [10] 已刪除　游能悌　2023/6/4 8:37:00 PM

第 6 頁: [11] 已刪除　游能悌　2023/3/13 2:18:00 PM

第 6 頁: [11] 已刪除　游能悌　2023/3/13 2:18:00 PM

第 6 頁: [11] 已刪除　游能悌　2023/3/13 2:18:00 PM

第 6 頁: [11] 已刪除　游能悌　2023/3/13 2:18:00 PM

第 6 頁: [11] 已刪除　游能悌　2023/3/13 2:18:00 PM

第 6 頁: [11] 已刪除　游能悌　2023/3/13 2:18:00 PM

第 6 頁: [11] 已刪除　游能悌　2023/3/13 2:18:00 PM

第 6 頁: [11] 已刪除　游能悌　2023/3/13 2:18:00 PM

第 6 頁: [11] 已刪除　游能悌　2023/3/13 2:18:00 PM

第 6 頁: [11] 已刪除　游能悌　2023/3/13 2:18:00 PM

第 6 頁: [11] 已刪除　游能悌　2023/3/13 2:18:00 PM

第 6 頁: [11] 已刪除　游能悌　2023/3/13 2:18:00 PM

第 6 頁: [11] 已刪除　游能悌　2023/3/13 2:18:00 PM

第 6 頁: [11] 已刪除　游能悌　2023/3/13 2:18:00 PM

第 6 頁: [11] 已刪除　游能悌　2023/3/13 2:18:00 PM

第 6 頁: [11] 已刪除　游能悌　2023/3/13 2:18:00 PM

第 6 頁: [11] 已刪除　游能悌　2023/3/13 2:18:00 PM

第 6 頁: [11] 已刪除　游能悌　2023/3/13 2:18:00 PM

第 6 頁: [11] 已刪除　游能悌　2023/3/13 2:18:00 PM

第 6 頁: [11] 已刪除　游能悌　2023/3/13 2:18:00 PM

第 6 頁: [11] 已刪除　游能悌　2023/3/13 2:18:00 PM

第 6 頁: [11] 已刪除　游能悌　2023/3/13 2:18:00 PM

第 6 頁: [11] 已刪除　游能悌　2023/3/13 2:18:00 PM

第 6 頁: [11] 已刪除　游能悌　2023/3/13 2:18:00 PM

第 6 頁: [11] 已刪除　游能悌　2023/3/13 2:18:00 PM

第 6 頁: [11] 已刪除　游能悌　2023/3/13 2:18:00 PM

第 6 頁: [11] 已刪除　游能悌　2023/3/13 2:18:00 PM

第 6 頁: [11] 已刪除　游能悌　2023/3/13 2:18:00 PM

第 6 頁: [12] 已刪除　游能悌　2023/6/2 5:13:00 PM

第 6 頁: [12] 已刪除　游能悌　2023/6/2 5:13:00 PM

第 6 頁: [12] 已刪除　游能悌　2023/6/2 5:13:00 PM

第 6 頁: [12] 已刪除　游能悌　2023/6/2 5:13:00 PM

第 6 頁: [12] 已刪除　游能悌　2023/6/2 5:13:00 PM

第 6 頁: [12] 已刪除　游能悌　2023/6/2 5:13:00 PM

第 6 頁: [12] 已刪除　游能悌　2023/6/2 5:13:00 PM

第 6 頁: [12] 已刪除　游能悌　2023/6/2 5:13:00 PM

第 6 頁: [12] 已刪除　游能悌　2023/6/2 5:13:00 PM

第 6 頁: [12] 已刪除　游能悌　2023/6/2 5:13:00 PM

第 6 頁: [12] 已刪除　游能悌　2023/6/2 5:13:00 PM

第 6 頁: [12] 已刪除　游能悌　2023/6/2 5:13:00 PM

第 6 頁: [12] 已刪除　游能悌　2023/6/2 5:13:00 PM

第 6 頁: [12] 已刪除　游能悌　2023/6/2 5:13:00 PM

第 6 頁: [12] 已刪除　游能悌　2023/6/2 5:13:00 PM

第 6 頁: [12] 已刪除　游能悌　2023/6/2 5:13:00 PM

第 6 頁: [12] 已刪除　游能悌　2023/6/2 5:13:00 PM

第 6 頁: [12] 已刪除　游能悌　2023/6/2 5:13:00 PM

第 6 頁: [12] 已刪除　游能悌　2023/6/2 5:13:00 PM

第 6 頁: [12] 已刪除　游能悌　2023/6/2 5:13:00 PM

第 6 頁: [12] 已刪除　游能悌　2023/6/2 5:13:00 PM

第 6 頁: [12] 已刪除　游能悌　2023/6/2 5:13:00 PM

第 6 頁: [12] 已刪除　游能悌　2023/6/2 5:13:00 PM

第 6 頁: [12] 已刪除　游能悌　2023/6/2 5:13:00 PM

第 6 頁: [12] 已刪除　游能悌　2023/6/2 5:13:00 PM

第 6 頁: [12] 已刪除　游能悌　2023/6/2 5:13:00 PM

第 6 頁: [12] 已刪除　游能悌　2023/6/2 5:13:00 PM

第 6 頁: [12] 已刪除　游能悌　2023/6/2 5:13:00 PM

第 6 頁: [13] 已刪除　游能悌　2023/6/10 2:35:00 PM

第 6 頁: [13] 已刪除　游能悌　2023/6/10 2:35:00 PM

第 6 頁: [13] 已刪除　游能悌　2023/6/10 2:35:00 PM

第 6 頁: [13] 已刪除　游能悌　2023/6/10 2:35:00 PM

第 6 頁: [13] 已刪除　游能悌　2023/6/10 2:35:00 PM

第 6 頁: [13] 已刪除　游能悌　2023/6/10 2:35:00 PM

第 6 頁: [13] 已刪除　游能悌　2023/6/10 2:35:00 PM

第 6 頁: [13] 已刪除　游能悌　2023/6/10 2:35:00 PM

第 6 頁: [13] 已刪除　游能悌　2023/6/10 2:35:00 PM

第 6 頁: [13] 已刪除　游能悌　2023/6/10 2:35:00 PM

第 6 頁: [13] 已刪除　游能悌　2023/6/10 2:35:00 PM

第 6 頁: [13] 已刪除　游能悌　2023/6/10 2:35:00 PM

第 6 頁: [13] 已刪除　游能悌　2023/6/10 2:35:00 PM

第 6 頁: [13] 已刪除　游能悌　2023/6/10 2:35:00 PM

第 6 頁: [14] 已刪除　游能悌　2023/6/10 2:38:00 PM

第 6 頁: [14] 已刪除　游能悌　2023/6/10 2:38:00 PM

第 6 頁: [14] 已刪除　游能悌　2023/6/10 2:38:00 PM

第 6 頁: [14] 已刪除　游能悌　2023/6/10 2:38:00 PM

第 11 頁: [15] 已刪除　游能悌　2023/6/3 1:31:00 PM

第 11 頁: [15] 已刪除　游能悌　2023/6/3 1:31:00 PM

第 11 頁: [15] 已刪除　游能悌　2023/6/3 1:31:00 PM

第 11 頁: [15] 已刪除　游能悌　2023/6/3 1:31:00 PM

第 11 頁: [15] 已刪除　游能悌　2023/6/3 1:31:00 PM

第 11 頁: [15] 已刪除　游能悌　2023/6/3 1:31:00 PM

第 11 頁: [15] 已刪除　游能悌　2023/6/3 1:31:00 PM

第 11 頁: [15] 已刪除　游能悌　2023/6/3 1:31:00 PM

第 11 頁: [15] 已刪除　游能悌　2023/6/3 1:31:00 PM

第 11 頁: [15] 已刪除　游能悌　2023/6/3 1:31:00 PM

第 11 頁: [15] 已刪除　游能悌　2023/6/3 1:31:00 PM

第 11 頁: [15] 已刪除　游能悌　2023/6/3 1:31:00 PM

第 11 頁: [15] 已刪除　游能悌　2023/6/3 1:31:00 PM

第 11 頁: [15] 已刪除　游能悌　2023/6/3 1:31:00 PM

第 11 頁: [15] 已刪除　游能悌　2023/6/3 1:31:00 PM

第 11 頁: [15] 已刪除　游能悌　2023/6/3 1:31:00 PM

第 11 頁: [16] 已刪除　游能悌　2023/3/15 4:41:00 PM

第 11 頁: [16] 已刪除　游能悌　2023/3/15 4:41:00 PM

第 11 頁: [16] 已刪除　游能悌　2023/3/15 4:41:00 PM

第 11 頁: [16] 已刪除　游能悌　2023/3/15 4:41:00 PM

第 11 頁: [16] 已刪除　游能悌　2023/3/15 4:41:00 PM

第 11 頁: [16] 已刪除　游能悌　2023/3/15 4:41:00 PM

第 11 頁: [16] 已刪除　游能悌　2023/3/15 4:41:00 PM

第 11 頁: [16] 已刪除　游能悌　2023/3/15 4:41:00 PM

第 11 頁: [17] 已刪除　游能悌　2023/6/10 2:57:00 PM

第 11 頁: [17] 已刪除　游能悌　2023/6/10 2:57:00 PM

第 11 頁: [17] 已刪除　游能悌　2023/6/10 2:57:00 PM

第 11 頁: [17] 已刪除　游能悌　2023/6/10 2:57:00 PM

第 11 頁: [17] 已刪除　游能悌　2023/6/10 2:57:00 PM

第 11 頁: [17] 已刪除　游能悌　2023/6/10 2:57:00 PM

第 11 頁: [17] 已刪除　游能悌　2023/6/10 2:57:00 PM

第 11 頁: [17] 已刪除　游能悌　2023/6/10 2:57:00 PM

第 11 頁: [17] 已刪除　游能悌　2023/6/10 2:57:00 PM

第 11 頁: [17] 已刪除　游能悌　2023/6/10 2:57:00 PM

第 11 頁: [17] 已刪除　游能悌　2023/6/10 2:57:00 PM

第 11 頁: [17] 已刪除　游能悌　2023/6/10 2:57:00 PM

第 12 頁: [18] 已刪除　游能悌　2023/5/23 9:18:00 AM

第 12 頁: [18] 已刪除　游能悌　2023/5/23 9:18:00 AM

第 12 頁: [18] 已刪除　游能悌　2023/5/23 9:18:00 AM

第 12 頁: [18] 已刪除　游能悌　2023/5/23 9:18:00 AM

第 12 頁: [18] 已刪除　游能悌　2023/5/23 9:18:00 AM

第 12 頁: [18] 已刪除　游能悌　2023/5/23 9:18:00 AM

第 12 頁: [18] 已刪除　游能悌　2023/5/23 9:18:00 AM

第 12 頁: [18] 已刪除　游能悌　2023/5/23 9:18:00 AM

第 12 頁: [19] 已刪除　游能悌　2023/5/31 5:33:00 PM

第 12 頁: [19] 已刪除　游能悌　2023/5/31 5:33:00 PM

第 12 頁: [19] 已刪除　游能悌　2023/5/31 5:33:00 PM

第 12 頁: [19] 已刪除　游能悌　2023/5/31 5:33:00 PM

第 12 頁: [19] 已刪除　游能悌　2023/5/31 5:33:00 PM

第 12 頁: [19] 已刪除　游能悌　2023/5/31 5:33:00 PM

第 12 頁: [19] 已刪除　游能悌　2023/5/31 5:33:00 PM

第 12 頁: [19] 已刪除　游能悌　2023/5/31 5:33:00 PM

第 12 頁: [19] 已刪除　游能悌　2023/5/31 5:33:00 PM

第 12 頁: [20] 已刪除　游能悌　2023/5/29 3:23:00 PM

第 12 頁: [20] 已刪除　游能悌　2023/5/29 3:23:00 PM

第 12 頁: [20] 已刪除　游能悌　2023/5/29 3:23:00 PM

第 12 頁: [20] 已刪除　游能悌　2023/5/29 3:23:00 PM

第 12 頁: [20] 已刪除　游能悌　2023/5/29 3:23:00 PM

第 12 頁: [20] 已刪除　游能悌　2023/5/29 3:23:00 PM

第 12 頁: [20] 已刪除　游能悌　2023/5/29 3:23:00 PM

第 12 頁: [20] 已刪除　游能悌　2023/5/29 3:23:00 PM

第 12 頁: [20] 已刪除　游能悌　2023/5/29 3:23:00 PM

第 12 頁: [20] 已刪除　游能悌　2023/5/29 3:23:00 PM

第 12 頁: [20] 已刪除　游能悌　2023/5/29 3:23:00 PM

第 12 頁: [20] 已刪除　游能悌　2023/5/29 3:23:00 PM

第 12 頁: [20] 已刪除　游能悌　2023/5/29 3:23:00 PM

第 12 頁: [20] 已刪除　游能悌　2023/5/29 3:23:00 PM

第 12 頁: [20] 已刪除　游能悌　2023/5/29 3:23:00 PM

第 12 頁: [20] 已刪除　游能悌　2023/5/29 3:23:00 PM

第 12 頁: [20] 已刪除　游能悌　2023/5/29 3:23:00 PM

第 13 頁: [21] 已刪除　游能悌　2023/5/31 5:49:00 PM

第 13 頁: [21] 已刪除　游能悌　2023/5/31 5:49:00 PM

第 13 頁: [21] 已刪除　游能悌　2023/5/31 5:49:00 PM

第 13 頁: [21] 已刪除　游能悌　2023/5/31 5:49:00 PM

第 13 頁: [22] 已刪除　游能悌　2023/5/31 5:57:00 PM

第 13 頁: [22] 已刪除　游能悌　2023/5/31 5:57:00 PM

第 13 頁: [22] 已刪除　游能悌　2023/5/31 5:57:00 PM

第 13 頁: [22] 已刪除　游能悌　2023/5/31 5:57:00 PM

第 13 頁: [22] 已刪除　游能悌　2023/5/31 5:57:00 PM

第 13 頁: [22] 已刪除　游能悌　2023/5/31 5:57:00 PM

第 13 頁: [22] 已刪除　游能悌　2023/5/31 5:57:00 PM

第 13 頁: [22] 已刪除　游能悌　2023/5/31 5:57:00 PM

第 13 頁: [22] 已刪除　游能悌　2023/5/31 5:57:00 PM

第 13 頁: [22] 已刪除　游能悌　2023/5/31 5:57:00 PM

第 13 頁: [22] 已刪除　游能悌　2023/5/31 5:57:00 PM

第 13 頁: [22] 已刪除　游能悌　2023/5/31 5:57:00 PM

第 13 頁: [22] 已刪除　游能悌　2023/5/31 5:57:00 PM

第 13 頁: [22] 已刪除　游能悌　2023/5/31 5:57:00 PM

第 13 頁: [22] 已刪除　游能悌　2023/5/31 5:57:00 PM

第 13 頁: [22] 已刪除　游能悌　2023/5/31 5:57:00 PM

第 13 頁: [22] 已刪除　游能悌　2023/5/31 5:57:00 PM

第 13 頁: [23] 已刪除　游能悌　2023/6/10 3:29:00 PM

第 13 頁: [23] 已刪除　游能悌　2023/6/10 3:29:00 PM

第 13 頁: [23] 已刪除　游能悌　2023/6/10 3:29:00 PM

第 13 頁: [23] 已刪除　游能悌　2023/6/10 3:29:00 PM

第 13 頁: [23] 已刪除　游能悌　2023/6/10 3:29:00 PM

第 13 頁: [23] 已刪除　游能悌　2023/6/10 3:29:00 PM

第 13 頁: [23] 已刪除　游能悌　2023/6/10 3:29:00 PM

第 13 頁: [23] 已刪除　游能悌　2023/6/10 3:29:00 PM

第 13 頁: [23] 已刪除　游能悌　2023/6/10 3:29:00 PM

第 13 頁: [23] 已刪除　游能悌　2023/6/10 3:29:00 PM

第 13 頁: [23] 已刪除　游能悌　2023/6/10 3:29:00 PM

第 13 頁: [23] 已刪除　游能悌　2023/6/10 3:29:00 PM

第 13 頁: [23] 已刪除　游能悌　2023/6/10 3:29:00 PM

第 13 頁: [23] 已刪除　游能悌　2023/6/10 3:29:00 PM

第 13 頁: [23] 已刪除　游能悌　2023/6/10 3:29:00 PM

第 13 頁: [23] 已刪除　游能悌　2023/6/10 3:29:00 PM

第 13 頁: [23] 已刪除　游能悌　2023/6/10 3:29:00 PM

第 13 頁: [23] 已刪除　游能悌　2023/6/10 3:29:00 PM

第 13 頁: [24] 已刪除　游能悌　2023/2/24 9:42:00 AM

第 13 頁: [24] 已刪除　游能悌　2023/2/24 9:42:00 AM

第 13 頁: [24] 已刪除　游能悌　2023/2/24 9:42:00 AM

第 13 頁: [25] 已刪除　游能悌　2023/6/4 9:56:00 PM

第 13 頁: [25] 已刪除　游能悌　2023/6/4 9:56:00 PM

第 13 頁: [25] 已刪除　游能悌　2023/6/4 9:56:00 PM

第 13 頁: [25] 已刪除　游能悌　2023/6/4 9:56:00 PM

第 13 頁: [25] 已刪除　游能悌　2023/6/4 9:56:00 PM

第 13 頁: [25] 已刪除　游能悌　2023/6/4 9:56:00 PM

第 13 頁: [25] 已刪除　游能悌　2023/6/4 9:56:00 PM

第 13 頁: [26] 已刪除　游能悌　2023/6/10 3:46:00 PM

第 13 頁: [26] 已刪除　游能悌　2023/6/10 3:46:00 PM

第 13 頁: [26] 已刪除　游能悌　2023/6/10 3:46:00 PM

第 13 頁: [26] 已刪除　游能悌　2023/6/10 3:46:00 PM

第 13 頁: [26] 已刪除　游能悌　2023/6/10 3:46:00 PM

第 13 頁: [26] 已刪除　游能悌　2023/6/10 3:46:00 PM

第 13 頁: [26] 已刪除　游能悌　2023/6/10 3:46:00 PM

第 13 頁: [26] 已刪除　游能悌　2023/6/10 3:46:00 PM

第 13 頁: [26] 已刪除　游能悌　2023/6/10 3:46:00 PM

第 13 頁: [26] 已刪除　游能悌　2023/6/10 3:46:00 PM

第 13 頁: [26] 已刪除　游能悌　2023/6/10 3:46:00 PM

第 13 頁: [26] 已刪除　游能悌　2023/6/10 3:46:00 PM

第 13 頁: [26] 已刪除　游能悌　2023/6/10 3:46:00 PM

第 13 頁: [26] 已刪除　游能悌　2023/6/10 3:46:00 PM

第 13 頁: [26] 已刪除　游能悌　2023/6/10 3:46:00 PM

第 13 頁: [26] 已刪除　游能悌　2023/6/10 3:46:00 PM

第 13 頁: [26] 已刪除　游能悌　2023/6/10 3:46:00 PM

第 15 頁: [27] 已刪除　游能悌　2023/6/3 2:45:00 PM

第 15 頁: [27] 已刪除　游能悌　2023/6/3 2:45:00 PM

第 15 頁: [27] 已刪除　游能悌　2023/6/3 2:45:00 PM

第 15 頁: [27] 已刪除　游能悌　2023/6/3 2:45:00 PM

第 15 頁: [27] 已刪除　游能悌　2023/6/3 2:45:00 PM

第 15 頁: [27] 已刪除　游能悌　2023/6/3 2:45:00 PM

第 15 頁: [27] 已刪除　游能悌　2023/6/3 2:45:00 PM

第 15 頁: [27] 已刪除　游能悌　2023/6/3 2:45:00 PM

第 15 頁: [27] 已刪除　游能悌　2023/6/3 2:45:00 PM

第 15 頁: [27] 已刪除　游能悌　2023/6/3 2:45:00 PM

第 15 頁: [27] 已刪除　游能悌　2023/6/3 2:45:00 PM

第 15 頁: [27] 已刪除　游能悌　2023/6/3 2:45:00 PM

第 15 頁: [27] 已刪除　游能悌　2023/6/3 2:45:00 PM

第 15 頁: [27] 已刪除　游能悌　2023/6/3 2:45:00 PM

第 15 頁: [27] 已刪除　游能悌　2023/6/3 2:45:00 PM

第 15 頁: [27] 已刪除　游能悌　2023/6/3 2:45:00 PM

第 15 頁: [27] 已刪除　游能悌　2023/6/3 2:45:00 PM

第 15 頁: [27] 已刪除　游能悌　2023/6/3 2:45:00 PM

第 15 頁: [27] 已刪除　游能悌　2023/6/3 2:45:00 PM

第 15 頁: [27] 已刪除　游能悌　2023/6/3 2:45:00 PM

第 15 頁: [27] 已刪除　游能悌　2023/6/3 2:45:00 PM

第 15 頁: [27] 已刪除　游能悌　2023/6/3 2:45:00 PM

第 15 頁: [27] 已刪除　游能悌　2023/6/3 2:45:00 PM

第 15 頁: [27] 已刪除　游能悌　2023/6/3 2:45:00 PM

第 15 頁: [27] 已刪除　游能悌　2023/6/3 2:45:00 PM

第 15 頁: [27] 已刪除　游能悌　2023/6/3 2:45:00 PM

第 15 頁: [27] 已刪除　游能悌　2023/6/3 2:45:00 PM

第 15 頁: [28] 已刪除　游能悌　2023/6/10 3:54:00 PM

第 15 頁: [28] 已刪除　游能悌　2023/6/10 3:54:00 PM

第 15 頁: [28] 已刪除　游能悌　2023/6/10 3:54:00 PM

第 15 頁: [28] 已刪除　游能悌　2023/6/10 3:54:00 PM

第 15 頁: [28] 已刪除　游能悌　2023/6/10 3:54:00 PM

第 15 頁: [29] 已刪除　游能悌　2023/5/28 1:30:00 PM

第 15 頁: [29] 已刪除　游能悌　2023/5/28 1:30:00 PM

第 15 頁: [29] 已刪除　游能悌　2023/5/28 1:30:00 PM

第 15 頁: [29] 已刪除　游能悌　2023/5/28 1:30:00 PM

第 15 頁: [29] 已刪除　游能悌　2023/5/28 1:30:00 PM

第 15 頁: [29] 已刪除　游能悌　2023/5/28 1:30:00 PM

第 15 頁: [29] 已刪除　游能悌　2023/5/28 1:30:00 PM

第 19 頁: [30] 已刪除　游能悌　2023/6/10 4:29:00 PM

第 19 頁: [30] 已刪除　游能悌　2023/6/10 4:29:00 PM

第 19 頁: [30] 已刪除　游能悌　2023/6/10 4:29:00 PM

第 19 頁: [30] 已刪除　游能悌　2023/6/10 4:29:00 PM

第 19 頁: [31] 已刪除　游能悌　2023/6/10 4:30:00 PM

第 19 頁: [31] 已刪除　游能悌　2023/6/10 4:30:00 PM

第 19 頁: [31] 已刪除　游能悌　2023/6/10 4:30:00 PM

第 19 頁: [31] 已刪除　游能悌　2023/6/10 4:30:00 PM

第 19 頁: [31] 已刪除　游能悌　2023/6/10 4:30:00 PM

第 19 頁: [31] 已刪除　游能悌　2023/6/10 4:30:00 PM

第 19 頁: [31] 已刪除　游能悌　2023/6/10 4:30:00 PM

第 19 頁: [31] 已刪除　游能悌　2023/6/10 4:30:00 PM

第 19 頁: [31] 已刪除　游能悌　2023/6/10 4:30:00 PM

第 19 頁: [31] 已刪除　游能悌　2023/6/10 4:30:00 PM

第 19 頁: [31] 已刪除　游能悌　2023/6/10 4:30:00 PM

第 19 頁: [31] 已刪除　游能悌　2023/6/10 4:30:00 PM

第 19 頁: [31] 已刪除　游能悌　2023/6/10 4:30:00 PM

第 19 頁: [32] 已刪除　游能悌　2023/6/3 2:59:00 PM

第 19 頁: [32] 已刪除　游能悌　2023/6/3 2:59:00 PM

第 19 頁: [32] 已刪除　游能悌　2023/6/3 2:59:00 PM

第 19 頁: [32] 已刪除　游能悌　2023/6/3 2:59:00 PM

第 19 頁: [32] 已刪除　游能悌　2023/6/3 2:59:00 PM

第 19 頁: [33] 已刪除　游能悌　2023/5/28 1:49:00 PM

第 19 頁: [33] 已刪除　游能悌　2023/5/28 1:49:00 PM

第 19 頁: [33] 已刪除　游能悌　2023/5/28 1:49:00 PM

第 19 頁: [33] 已刪除　游能悌　2023/5/28 1:49:00 PM

第 19 頁: [33] 已刪除　游能悌　2023/5/28 1:49:00 PM

第 19 頁: [33] 已刪除　游能悌　2023/5/28 1:49:00 PM

第 19 頁: [33] 已刪除　游能悌　2023/5/28 1:49:00 PM

第 19 頁: [33] 已刪除　游能悌　2023/5/28 1:49:00 PM

第 19 頁: [33] 已刪除　游能悌　2023/5/28 1:49:00 PM

第 19 頁: [33] 已刪除　游能悌　2023/5/28 1:49:00 PM

第 19 頁: [33] 已刪除　游能悌　2023/5/28 1:49:00 PM

第 19 頁: [33] 已刪除　游能悌　2023/5/28 1:49:00 PM

第 19 頁: [33] 已刪除　游能悌　2023/5/28 1:49:00 PM

第 19 頁: [33] 已刪除　游能悌　2023/5/28 1:49:00 PM

第 19 頁: [33] 已刪除　游能悌　2023/5/28 1:49:00 PM

第 19 頁: [33] 已刪除　游能悌　2023/5/28 1:49:00 PM

第 19 頁: [33] 已刪除　游能悌　2023/5/28 1:49:00 PM

第 19 頁: [34] 已刪除　游能悌　2023/5/24 10:39:00 AM

第 19 頁: [34] 已刪除　游能悌　2023/5/24 10:39:00 AM

第 19 頁: [34] 已刪除　游能悌　2023/5/24 10:39:00 AM

第 19 頁: [34] 已刪除　游能悌　2023/5/24 10:39:00 AM

第 19 頁: [34] 已刪除　游能悌　2023/5/24 10:39:00 AM

第 19 頁: [34] 已刪除　游能悌　2023/5/24 10:39:00 AM

第 19 頁: [34] 已刪除　游能悌　2023/5/24 10:39:00 AM

第 19 頁: [34] 已刪除　游能悌　2023/5/24 10:39:00 AM

第 19 頁: [34] 已刪除　游能悌　2023/5/24 10:39:00 AM

第 19 頁: [34] 已刪除　游能悌　2023/5/24 10:39:00 AM

第 19 頁: [34] 已刪除　游能悌　2023/5/24 10:39:00 AM

第 19 頁: [35] 已刪除　游能悌　2023/5/24 10:41:00 AM

第 19 頁: [35] 已刪除　游能悌　2023/5/24 10:41:00 AM

第 19 頁: [35] 已刪除　游能悌　2023/5/24 10:41:00 AM

第 19 頁: [35] 已刪除　游能悌　2023/5/24 10:41:00 AM

第 19 頁: [36] 已刪除　游能悌　2023/5/24 10:42:00 AM

第 19 頁: [36] 已刪除　游能悌　2023/5/24 10:42:00 AM

第 19 頁: [36] 已刪除　游能悌　2023/5/24 10:42:00 AM

第 19 頁: [36] 已刪除　游能悌　2023/5/24 10:42:00 AM

第 19 頁: [36] 已刪除　游能悌　2023/5/24 10:42:00 AM

第 19 頁: [36] 已刪除　游能悌　2023/5/24 10:42:00 AM

第 19 頁: [36] 已刪除　游能悌　2023/5/24 10:42:00 AM

第 19 頁: [36] 已刪除　游能悌　2023/5/24 10:42:00 AM

第 19 頁: [36] 已刪除　游能悌　2023/5/24 10:42:00 AM

第 19 頁: [36] 已刪除　游能悌　2023/5/24 10:42:00 AM

第 19 頁: [36] 已刪除　游能悌　2023/5/24 10:42:00 AM

第 19 頁: [36] 已刪除　游能悌　2023/5/24 10:42:00 AM

第 19 頁: [36] 已刪除　游能悌　2023/5/24 10:42:00 AM

第 19 頁: [36] 已刪除　游能悌　2023/5/24 10:42:00 AM

第 19 頁: [36] 已刪除　游能悌　2023/5/24 10:42:00 AM

第 19 頁: [36] 已刪除　游能悌　2023/5/24 10:42:00 AM

第 19 頁: [36] 已刪除　游能悌　2023/5/24 10:42:00 AM

第 19 頁: [36] 已刪除　游能悌　2023/5/24 10:42:00 AM

第 19 頁: [36] 已刪除　游能悌　2023/5/24 10:42:00 AM

第 19 頁: [36] 已刪除　游能悌　2023/5/24 10:42:00 AM

第 19 頁: [36] 已刪除　游能悌　2023/5/24 10:42:00 AM

第 22 頁: [37] 已刪除　游能悌　2023/5/24 11:52:00 AM

第 22 頁: [37] 已刪除　游能悌　2023/5/24 11:52:00 AM

第 22 頁: [37] 已刪除　游能悌　2023/5/24 11:52:00 AM

第 22 頁: [38] 已刪除　游能悌　2023/5/24 11:53:00 AM

第 22 頁: [38] 已刪除　游能悌　2023/5/24 11:53:00 AM

第 22 頁: [38] 已刪除　游能悌　2023/5/24 11:53:00 AM

第 22 頁: [38] 已刪除　游能悌　2023/5/24 11:53:00 AM

第 22 頁: [38] 已刪除　游能悌　2023/5/24 11:53:00 AM

第 22 頁: [38] 已刪除　游能悌　2023/5/24 11:53:00 AM

第 22 頁: [38] 已刪除　游能悌　2023/5/24 11:53:00 AM

第 22 頁: [38] 已刪除　游能悌　2023/5/24 11:53:00 AM

第 22 頁: [38] 已刪除　游能悌　2023/5/24 11:53:00 AM

第 22 頁: [38] 已刪除　游能悌　2023/5/24 11:53:00 AM

第 22 頁: [38] 已刪除　游能悌　2023/5/24 11:53:00 AM

第 22 頁: [38] 已刪除　游能悌　2023/5/24 11:53:00 AM

第 22 頁: [38] 已刪除　游能悌　2023/5/24 11:53:00 AM

第 22 頁: [38] 已刪除　游能悌　2023/5/24 11:53:00 AM

第 22 頁: [38] 已刪除　游能悌　2023/5/24 11:53:00 AM

第 22 頁: [39] 已設定格式　游能悌　2023/6/4 10:31:00 PM

上標

第 22 頁: [39] 已設定格式　游能悌　2023/6/4 10:31:00 PM

上標

第 22 頁: [40] 已刪除　游能悌　2023/6/4 10:32:00 PM

第 22 頁: [40] 已刪除　游能悌　2023/6/4 10:32:00 PM

第 22 頁: [40] 已刪除　游能悌　2023/6/4 10:32:00 PM

第 22 頁: [40] 已刪除　游能悌　2023/6/4 10:32:00 PM

第 22 頁: [40] 已刪除　游能悌　2023/6/4 10:32:00 PM

第 22 頁: [40] 已刪除　游能悌　2023/6/4 10:32:00 PM

第 22 頁: [40] 已刪除　游能悌　2023/6/4 10:32:00 PM

第 22 頁: [40] 已刪除　游能悌　2023/6/4 10:32:00 PM

第 22 頁: [40] 已刪除　游能悌　2023/6/4 10:32:00 PM

第 22 頁: [41] 已刪除　游能悌　2023/6/4 10:35:00 PM

第 22 頁: [41] 已刪除　游能悌　2023/6/4 10:35:00 PM

第 22 頁: [41] 已刪除　游能悌　2023/6/4 10:35:00 PM

第 22 頁: [41] 已刪除　游能悌　2023/6/4 10:35:00 PM

第 22 頁: [41] 已刪除　游能悌　2023/6/4 10:35:00 PM

第 22 頁: [41] 已刪除　游能悌　2023/6/4 10:35:00 PM

第 22 頁: [41] 已刪除　游能悌　2023/6/4 10:35:00 PM

第 22 頁: [41] 已刪除　游能悌　2023/6/4 10:35:00 PM

第 22 頁: [41] 已刪除　游能悌　2023/6/4 10:35:00 PM

第 22 頁: [41] 已刪除　游能悌　2023/6/4 10:35:00 PM

第 22 頁: [41] 已刪除　游能悌　2023/6/4 10:35:00 PM

第 22 頁: [41] 已刪除　游能悌　2023/6/4 10:35:00 PM

第 22 頁: [41] 已刪除　游能悌　2023/6/4 10:35:00 PM

第 22 頁: [41] 已刪除　游能悌　2023/6/4 10:35:00 PM

第 22 頁: [41] 已刪除　游能悌　2023/6/4 10:35:00 PM

第 22 頁: [41] 已刪除　游能悌　2023/6/4 10:35:00 PM

第 22 頁: [41] 已刪除　游能悌　2023/6/4 10:35:00 PM

第 22 頁: [41] 已刪除　游能悌　2023/6/4 10:35:00 PM

第 22 頁: [41] 已刪除　游能悌　2023/6/4 10:35:00 PM

第 22 頁: [42] 已刪除　游能悌　2023/5/25 3:36:00 PM

第 22 頁: [42] 已刪除　游能悌　2023/5/25 3:36:00 PM

第 22 頁: [42] 已刪除　游能悌　2023/5/25 3:36:00 PM

第 22 頁: [42] 已刪除　游能悌　2023/5/25 3:36:00 PM

第 23 頁: [43] 已刪除　游能悌　2023/6/3 3:41:00 PM

第 23 頁: [43] 已刪除　游能悌　2023/6/3 3:41:00 PM

第 23 頁: [44] 已刪除　游能悌　2023/5/25 3:42:00 PM

第 23 頁: [44] 已刪除　游能悌　2023/5/25 3:42:00 PM

第 23 頁: [44] 已刪除　游能悌　2023/5/25 3:42:00 PM

第 23 頁: [44] 已刪除　游能悌　2023/5/25 3:42:00 PM

第 23 頁: [44] 已刪除　游能悌　2023/5/25 3:42:00 PM

第 23 頁: [44] 已刪除　游能悌　2023/5/25 3:42:00 PM

第 23 頁: [44] 已刪除　游能悌　2023/5/25 3:42:00 PM

第 23 頁: [44] 已刪除　游能悌　2023/5/25 3:42:00 PM

第 23 頁: [44] 已刪除　游能悌　2023/5/25 3:42:00 PM

第 23 頁: [44] 已刪除　游能悌　2023/5/25 3:42:00 PM

第 23 頁: [44] 已刪除　游能悌　2023/5/25 3:42:00 PM

第 23 頁: [44] 已刪除　游能悌　2023/5/25 3:42:00 PM

第 23 頁: [44] 已刪除　游能悌　2023/5/25 3:42:00 PM

第 23 頁: [44] 已刪除　游能悌　2023/5/25 3:42:00 PM

第 23 頁: [44] 已刪除　游能悌　2023/5/25 3:42:00 PM

第 23 頁: [44] 已刪除　游能悌　2023/5/25 3:42:00 PM

第 23 頁: [44] 已刪除　游能悌　2023/5/25 3:42:00 PM

第 23 頁: [44] 已刪除　游能悌　2023/5/25 3:42:00 PM

第 23 頁: [44] 已刪除　游能悌　2023/5/25 3:42:00 PM

第 23 頁: [44] 已刪除　游能悌　2023/5/25 3:42:00 PM

第 23 頁: [44] 已刪除　游能悌　2023/5/25 3:42:00 PM

第 23 頁: [45] 已刪除　游能悌　2023/6/3 3:43:00 PM

第 23 頁: [45] 已刪除　游能悌　2023/6/3 3:43:00 PM

第 23 頁: [45] 已刪除　游能悌　2023/6/3 3:43:00 PM

第 23 頁: [45] 已刪除　游能悌　2023/6/3 3:43:00 PM

第 23 頁: [45] 已刪除　游能悌　2023/6/3 3:43:00 PM

第 23 頁: [45] 已刪除　游能悌　2023/6/3 3:43:00 PM

第 23 頁: [45] 已刪除　游能悌　2023/6/3 3:43:00 PM

第 23 頁: [45] 已刪除　游能悌　2023/6/3 3:43:00 PM

第 23 頁: [45] 已刪除　游能悌　2023/6/3 3:43:00 PM

第 23 頁: [45] 已刪除　游能悌　2023/6/3 3:43:00 PM

第 23 頁: [45] 已刪除　游能悌　2023/6/3 3:43:00 PM

第 23 頁: [45] 已刪除　游能悌　2023/6/3 3:43:00 PM

第 23 頁: [45] 已刪除　游能悌　2023/6/3 3:43:00 PM

第 23 頁: [45] 已刪除　游能悌　2023/6/3 3:43:00 PM

第 23 頁: [45] 已刪除　游能悌　2023/6/3 3:43:00 PM

第 23 頁: [45] 已刪除　游能悌　2023/6/3 3:43:00 PM

第 23 頁: [46] 已刪除　游能悌　2023/6/10 4:48:00 PM

第 23 頁: [46] 已刪除　游能悌　2023/6/10 4:48:00 PM

第 23 頁: [46] 已刪除　游能悌　2023/6/10 4:48:00 PM

第 23 頁: [46] 已刪除　游能悌　2023/6/10 4:48:00 PM

第 23 頁: [46] 已刪除　游能悌　2023/6/10 4:48:00 PM

第 23 頁: [46] 已刪除　游能悌　2023/6/10 4:48:00 PM

第 23 頁: [46] 已刪除　游能悌　2023/6/10 4:48:00 PM

第 23 頁: [46] 已刪除　游能悌　2023/6/10 4:48:00 PM
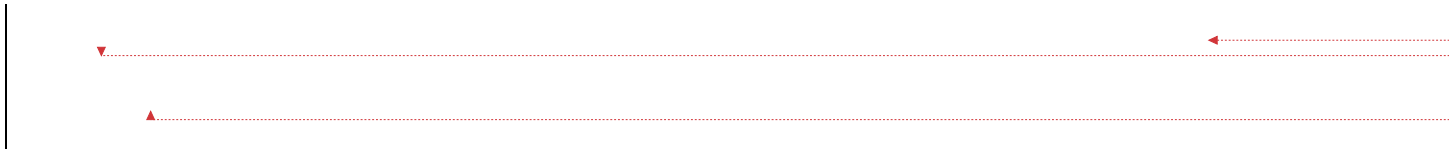
第 23 頁: [46] 已刪除　游能悌　2023/6/10 4:48:00 PM